SIMULATION OF THE OIL-WATER INVERSION PROCESS

By

JUSTIN JUSWANDI

Bachelor of Science

Oklahoma State University

Stillwater, Oklahoma

1993

Submitted to the Faculty of the
Graduate College of the
Oklahoma State University
in partial fulfillment of
the requirements for
the Degree of
MASTER OF SCIENCE
May, 1995

SIMULATION OF THE OIL-WATER

INVERSION PROCESS

Thesis Approved:

Alan Sue

Thesis Advisor

Mark S. Hyl

Robert S. Robinson Jr.

Thomas C. Collins

Dean of the Graduate College

ACKNOWLEDGMENTS

I wish to express my sincere appreciation to my advisor, Dr. Alan D. Tree for his guidance, motivation, and inspiration throughout this study. I also appreciate his patience in going through my thesis corrections. I am also thankful to my other committee members, Dr. Martin High and Dr. Robert L. Robinson, Jr. for their support and encouragement.

I wish to express gratitude to those who provided suggestions and assistance in this study: Dr. Guohai Liu, Mr. Sivakumar Sambasivam, Mr. Xiaofeng Guan, and Mr. Lim Khian Thong.

I would also like to give my special appreciation to my mom, brothers, sister, and all my relatives who have always provided me with their everlasting support and encouragement.

Finally, I would like to thank all the industrial sponsors and School of Chemical Engineering for their financial support during this study.

TABLE OF CONTENTS

LIST OF TABLES

LIST OF FIGURES

CHAPTER I

INTRODUCTION

Corrosion is a serious problem in gas and oil production. Corrosion causes an increase in production cost due to the additional spending on corrosion controls. Loss of production can also occur in a severely corroded well due to downtime. The expense associated with corrosion has led to continuous research to understand the nature of corrosion in gas and oil wells and to find more effective ways to prevent the corrosion.

Corrosion in oil and gas wells is generally controlled by the use of corrosion resistant metals, protective coatings, and inhibitors. The type of corrosion control used in a particular well depends on the conditions in the well. Sometimes, two or more corrosion control methods are implemented in a single well in order to provide better protection.

The most reliable method to control corrosion is to use corrosion resistant metals. However, the cost of the corrosion resistant metals is very high and is generally too expensive.

A more affordable but less reliable method is to use protective coatings. The coatings can be plastic,

inorganic, metallic, and non-metallic materials. The drawback of using protective coatings is that they have to be free of any defect since a small defect may spread quickly and cause a rapid failure.

Inhibitors are also used to protect gas and oil wells. Inhibitors are generally organic chemicals which adhere to the surface of the metal and promote the formation of an oil film which protects the metal. However, in order for an inhibitor to be effective in protecting the metal, it has to cover all the metal surfaces, which is difficult to accomplish in practice.

To reduce the cost of corrosion controls and to protect gas and oil wells more effectively, the ability to predict the location where corrosion begins is valuable. The ability to make such a prediction has the potential of saving capital and operating costs because the use of corrosion resistant metals, protective coatings, or inhibitors can be greatly reduced. In this project, a model to predict the conditions under which corrosion begins has been developed.

The presence of water in contact with the metal on the tube wall is necessary for the corrosion to occur. The water may contain dissolved CO_2 or H_2S which is acidic and corrosive to most metals.

Predicting the location where water first wets the metal in a gas well is the goal in this project. The flow of gas and liquid inside a gas well is very turbulent and

chaotic. An annular flow typically exists in a gas well. The gas flows in the core and the liquid film flows on the tube wall. The liquid film consists of oil and water which are present as an emulsion. Due to the immicibility of oil and water, one phase is dispersed in the other. Near the bottom of the well, liquid water is usually present in a small amount, therefore, water is initially dispersed in the oil. The amount of water condensate in the film increases in the upper part of the well due to the temperature drop. At a certain point in the well, the volume fraction of water reaches a critical value and the water inverts to become the continuous phase and wets the metal. This process is called phase inversion.

No experimental work has been done to allow the prediction of phase inversion in the annular flow. Conducting an experiment in a laboratory to mimic the condition in gas wells will be very difficult. In this project, a computer simulation is used to study the phase inversion in gas wells.

CHAPTER II

LITERATURE REVIEW

All topics relevant and important to the development of the model will be reviewed here. Specifically, a review of downhole corrosion, emulsions, droplet coalescence, droplet breakup, drop size distribution, and computer simulation will be presented in this chapter.

Downhole Corrosion

Many factors have been found to affect the corrosion rate in gas and oil wells. Bacon and Brown (1943) found that a highly turbulent two-phase flow downstream of various fittings and orifice plates caused corrosion due to corrosion-erosion effects. Other factors that affect the corrosion rate include the partial pressure of CO_2 and H_2S present in gas phase, temperature, properties of the corrosion product film, fluid velocity, the type of flow regime, concentration of various inorganic ions in the formation water, and gas and water production rate.

Several researchers (Shock and Sudbury, 1951, Tuttle, 1987) indicated that the partial pressure of CO_2 and H_2S had a strong effect on corrosion by affecting the pH of water found in oil and gas field. As a rule of thumb, a well was

classified as corrosive if the partial pressure of the corrosive gases was above 15 psi. If the partial pressure of the corrosive gases was between 7 and 15 psi, the well was classified as probably corrosive. When the partial pressure of the corrosive gases was below 7 psi, the well was most likely non-corrosive.

Temperature affects the corrosion rate in gas and oil wells by changing the pH, the solubility of CO_2 in water, the electrochemical anodic and cathodic reaction rates, and by the formation of corrosion product layer. DeWaard et al. (1975) found that corrosion rate depended on temperature in an exponential manner, much like the exponential relationship in the Arrhenius equation. However, at higher temperature and higher partial pressure of CO_2, the corrosion rate did not depend on the temperature as strongly as predicted by DeWaard et al.

The deviation from the exponential relationship was due to the formation of corrosion product layer which partially protected the well. Ikeda (1984) found that at temperatures below 60 °C, the corrosion product layer that formed on the surface of the metal was soft and non-adhesive. At temperatures near 100 °C, the corrosion product layer was thick and loose. The corrosion rate was a maximum in this temperature range. At temperatures above 150 °C, the corrosion rate was found to be a minimum due to the formation of a fine, tight, adhesive film on the surface of the metal which prevented the metal from corroding further.

Another important factor that affects corrosion rate is the flow velocity. Choi, Cepulis, and Lee (1989) found that as the fluid velocity increased in water-in-oil (w/o) or oil-in-water (o/w) emulsion, the corrosion rate also increased. They argued that in the oil-continuous phase, the fluid velocity increased both the local turbulence and the contact time of the water phase with the metal. In the water-continuous phase, the increase in fluid velocity was claimed to have washed off the protective corrosion product and to have increased the mass transfer through the pores of the film.

The flow regime also affects the corrosion rate. Johnson et al. (1991) found that in slug flow the corrosion rate could be as high as seven times that in annular flow.

Chemical species in the formation water had also been found to affect the corrosion rate. Chloride ion with the presence of oxygen had been shown to greatly increase the localized corrosion. However, in the absence of oxygen, chloride ion actually reduced the uniform corrosion by surface inhibition. Chemical species that increased the alkalinity of the formation water were found to reduce the corrosion rate.

Water and gas production rate has a great influence on the corrosion rate as well. Bradburn (1977) observed that the water production rate was a better indicator of the corrosiveness of gas wells than the partial pressure of CO_2. The effect of gas production rate was later considered by

Gatzke and Hausler (1984) who found that the corrosion rate increased when the water or gas production increased.

Robertson and Erbar (1988) assumed that corrosion is most likely to occur in the water condensation zone. They developed a model to predict the water condensation zone in gas wells. The model took into account the two-phase flow regime and non-linear pressure drop in gas wells.

Liu and Erbar (1990) first developed a model which includes fluid mechanics, mass transfer, and surface reactions to predict uniform corrosion rates without protective films. In their model, the key corrosive species was hydrogen ion in the aqueous medium. The model also assumed that corrosion began at the location where condensation first occurred. Liu (1991) later modified the model to include the calculation of corrosion rate in the presence of protective films.

Sambasivam (1992) developed a computer model to predict the conditions under which corrosion was most likely to occur in gas wells. The model assumed that corrosion began when water actually wet the metal as opposed to when water condensation occurred. Sambasivam's model used a stochastic simulation (Monte Carlo method). Given the flow conditions, the model generated drop size distributions for both water-in-oil (w/o) and oil-in-water (o/w) emulsions. The energy of both type of emulsions was then calculated and compared. The emulsion with the lowest energy was taken as the stable emulsion. The volume fraction of water in the emulsion was

then increased and simulation was repeated until phase inversion occurred. Some problems were encountered in his model. The problems are listed below:

1. The simulation could only be performed with the ratio of maximum to minimum diameter of two;
2. Phase inversion always occurred at 0.5 volume fraction of water; and
3. The phase inversion did not depend on the physical properties of the system.

The project reported here continued Sambasivam's work and corrected these problems.

Emulsions

An emulsion is a dispersion of oil droplets in water (o/w) or water droplets in oil (w/o). In this document, any highly polar, hydrophilic liquid is categorized as water, and any non polar, hydrophobic liquid is categorized as oil.

Lissant (1974) argued that the behavior of emulsions depended more on their physical and topological configuration than on the chemical properties of their constituents. He divided emulsions into three categories. The first category was the emulsions with less than 30% volume of dispersed phase. The droplets in this type of emulsions did not have a close interaction with each other because of the large space between them. The property of the emulsion was determined mainly by the property of the continuous phase. Emulsions with 30% to about 74% volume of

dispersed phase fell into the second category. The droplets in this category had more collisions or interactions with each other. The close interactions of the droplets caused an increase in the viscosity of the emulsion. The third category was emulsions with more than 74% volume of dispersed phase. The emulsions in this category were usually unstable to shear unless special emulsifiers were used.

Stability of Emulsions

Emulsions are formed as a result of two competing processes: droplet coalescence and droplet breakup. Droplet coalescence is a natural process because it reduces the surface area, and therefore lowers the energy of the system. On the other hand, droplet breakup requires energy. Therefore, emulsions are thermodynamically unstable.

Emulsions can breakdown in several ways. One way is by the separation of the dispersed and continuous phases into two layers. Another way is by "creaming". Creaming is characterized by the formation of two different emulsion systems: an oil-rich system and an oil-poor system.

To form a stable emulsion, droplet coalescence has to be prevented. Emulsifiers are generally used to prevent droplet coalescence. Lissant (1974) stated that emulsions with small volume fraction of the dispersed phase were stabilized by using ionic emulsifiers and by producing very small droplets. For emulsions with higher volume fractions

of the dispersed phase, emulsifiers which formed thin film around the droplets were found to be more effective in stabilizing the emulsion.

Viscosity of Emulsions

Viscosity of emulsions is a very important physical property because it affects the stability of emulsions. The viscosity of an emulsion depends on the viscosity of the continuous phase, the volume fraction of the dispersed phase, and the droplet size distribution, as well as the temperature.

High viscosity in the continuous phase is found to stabilize an emulsion. Droplets in this system move slower because they experience greater resistance in the continuous phase. Slower movement of the droplets results in less droplet collision. Therefore, less droplet coalescence occurs and the emulsion is stable.

An increase in temperature reduces the viscosity of emulsion. The decrease in the viscosity results in an increase of droplet mobility. Consequently, the rate of droplet coalescence increases and the emulsion becomes less stable.

An increase in the volume fraction of the dispersed phase is found to increase the viscosity of the emulsion. However, the increase in the viscosity of emulsion due to the increase in the volume fraction of dispersed phase destabilizes the emulsion instead of stabilizing it.

Droplets which are close together in this type of system are more likely to collide and coalesce.

Droplet size has less effect on the viscosity of the emulsion than the other factors discussed above. Emulsions with smaller droplet sizes are found to be more viscous than the ones with larger droplet sizes. The stability of the emulsion is also increased by using smaller droplets with uniform size.

Phase Inversion

Emulsions can be inverted from one type to the other. In phase inversion, the dispersed phase inverts to become the continuous phase and vice versa.

Many factors can influence phase inversion. Lissant (1974) stated that phase inversion occurs when the volume fraction of the dispersed phase reached a critical value. Shinoda and Kunieda (1983) observed that phase inversion occurred at a certain temperature range which they called phase inversion temperature (PIT). Emulsions with temperature above the PIT were water-in-oil type and those with temperature below PIT were oil-in-water type. Smith, Covatch, and Lim (1991) observed that at a certain range of concentration, emulsions were always water-in-oil type and at another range they were always oil-in-water type. This observation contradicted the report of Shinoda and Kunieda.

Bhatnagar (1920) found that emulsifiers also affected phase inversion. He observed that trivalent electrolytes

were more effective than bivalent electrolytes in causing phase inversion.

Chemical species can also affect phase inversion. Simon and Poynter (1968) were able to invert highly viscous w/o emulsion to o/w by chemical means.

Mao and Marsden (1977) found that the inversion could also be achieved by varying oil concentration, temperature, and shear stress. Increasing the oil concentration and the temperature of an emulsion favored the formation of w/o emulsion. Increasing shear stress also favored the formation of w/o emulsion but its effect was negligible at high temperature.

Brooks and Richmond (1994) examined the effect of oil-phase viscosity and stirrer speed on phase inversion. They found that as the oil viscosity increased, the volume fraction of water required for the phase inversion decreased. The turbulence in the liquid was found to have less effect on phase inversion. They found that the volume fraction of water required for the inversion increased only slightly as the stirrer speed was increased.

Droplet Coalescence and Breakup

Droplets in an emulsion have different sizes. The drop size distribution exists because of the coalescence and breakup of droplets in the emulsion. The processes and mechanisms of droplet coalescence and breakup are still not fully understood.

Taylor (1934) studied droplet deformation and breakup under shear and extensional flows. He derived an equation to calculate the maximum drop diameter that could exist in a given flow condition:

$$d_{\max} = \frac{\sigma}{a\mu_c}\left[(16\mu_d + 16\mu_c)/(19\mu_d + 16\mu_c)\right] \qquad \text{(II-1)}$$

where d_{max} is the maximum drop diameter, a is the maximum velocity gradient in the flow field, σ is the interfacial tension, and μ_c and μ_d are the viscosity of the continuous and dispersed phase, respectively.

Clay (1940) obtained drop size distribution data produced in a turbulent pipe flow. He used his data to propose mechanisms for droplet coalescence and breakup. He observed that droplets coalesced on collision or after they clung to each other for some time. He suggested that a droplet brokeup because of a velocity gradient or a pressure difference on the surface of the droplet.

Kolmogoroff (1949) and Hinze (1955) studied droplet breakup based on the balance between two forces: the external forces which deformed the droplet and the interfacial tension forces which counteracted the deformation. Hinze defined a Weber number (We) as the ratio of the external forces to the interfacial tension forces:

$$We = \frac{\tau}{(\sigma / d)} \qquad \text{(II-2)}$$

where τ is the turbulent stresses, σ is the interfacial tension, and d is the diameter of the droplet. Kolmogoroff and Hinze also postulated that for a given flow condition a critical Weber number (We_{crit}) existed. If We of the droplet was greater than We_{crit} the droplet brokeup. Therefore, We_{crit} was defined as follows:

$$We_{crit} = \frac{\tau}{\sigma / d_{\max}} \qquad \text{(II-3)}$$

where d_{max} is the maximum stable diameter. Hinze showed that We_{crit} varied for different types of flow and deformation. Using Clay's data, he found that We_{crit} for droplets produced in turbulent pipe flow was about 1.

Kolmogoroff and Hinze suggested that in turbulent flow the spectrum of eddies which could break the droplet should have the size in the same order as the droplet diameter. Eddies with size much greater than the drop diameter could only translate the droplet. Eddies with size smaller than the drop diameter caused only small deformation which could not result in droplet breakup. Based on the above notion and equation (II-3), Hinze derived an equation to calculate the maximum stable diameter:

$$d_{\max} = (We_{crit} / 2)^{0.6} (\sigma / \rho_c)^{0.6} \varepsilon^{-0.4} \qquad \text{(II-4)}$$

where ε is the local energy dissipation per unit mass.

Levich (1962) derived an equation to calculate d_{max} based on the balance of the internal pressure of the drop

with the capillary pressure of the deformed drop. For flow in the tube, the equation is given by:

$$d_{max} = (\sigma / k_f \rho v^2)^{0.6} \lambda_0^{1.6} \qquad \text{(II-5)}$$

where k_f is a numerical constant, v is the kinematic viscosity, λ_o is the scale of eddy at which the Reynolds number is unity, ρ is the density of continuous phase.

Levich postulated that for pipe flow, droplets with the minimum diameter were found near the wall because it was the region where rapid changes in velocity occurred. The equation for the minimum diameter derived by Levich is given below:

$$d_{min} = (\sigma v / 25 \rho \upsilon_o^3) \qquad \text{(II-6)}$$

where υ_o is the characteristic eddy velocity.

Drop Size Distribution in Emulsions

Studies on emulsification processes and properties require the knowledge of drop size distribution. Experimental data of drop size distribution had shown that there was no general drop size distribution for all emulsions. The data suggested that the drop size distribution depended on how the emulsions were made.

Schwarz and Bezemer (1956) proposed a drop size distribution which was derived statistically. The equation which contains two parameters was found to agree with experimental data of emulsions which were prepared mechanically, but not with those prepared by phase

inversion, vapor condensation, or electrical disintegration. Schwarz and Bezemer found that drop size distributions of viscous paraffin in a Na Oleate solution and water in Schoonebeck crude oil were log-normally distributed. The drop size distributions are shown in Figure 1 and 2. The maximums of the distributions in Figure 1 and 2 are skewed to the left.

Collins and Knudsen (1970) experimentally obtained the drop size distribution of oil-in-water in a well defined turbulent pipe flow. The drop size distribution is given in Figure 3. The drop size distribution did not follow any kind of known distributions, such as log-normal, upper-limit log normal, etc. They argued that the drop size distribution measured was actually a superposition of two distributions, one was initially present and the other produced by turbulence in the flow field.

Karabelas (1978) measured the drop size distribution of water in two liquid hydrocarbons of viscosity approximately 2 and 20 mNs/m^2 in pipe flow. He found the distribution could be fitted to an upper-limit log normal function.

The Monte Carlo Method

Computer simulation has been used to solve various problems in engineering. Data from experiments can be compared to the results from the computer simulation. If the comparison is good, the computer simulation can be used to provide insight into the experiment or used to predict

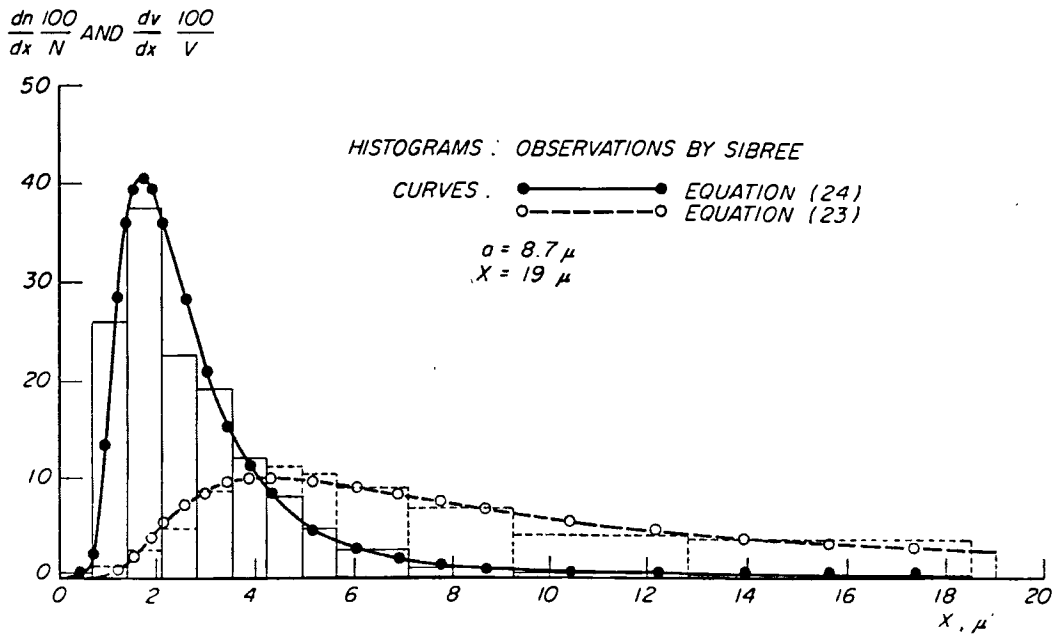

Figure 1:
Drop Size Distribution of Viscous Paraffin in Na Oleate Solution (Taken from Kolloid Zeitschrift 1956, Vol. 146, p. 142)

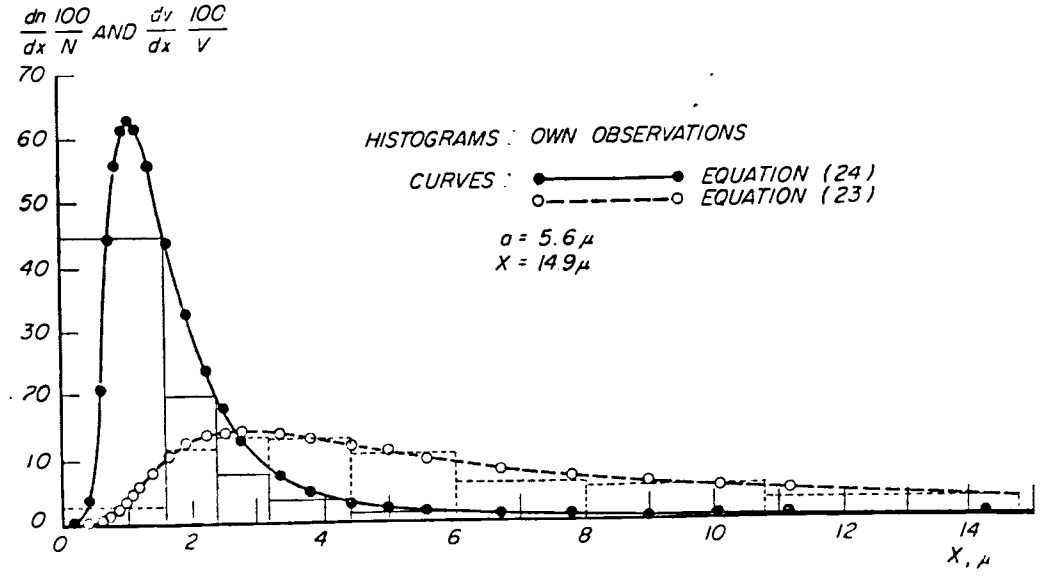

Figure 2:
Drop Size Distribution of Water in Schoonebeck Crude Oil (Taken from Kolloid Zeitschrift 1956, Vol. 146, p. 143)

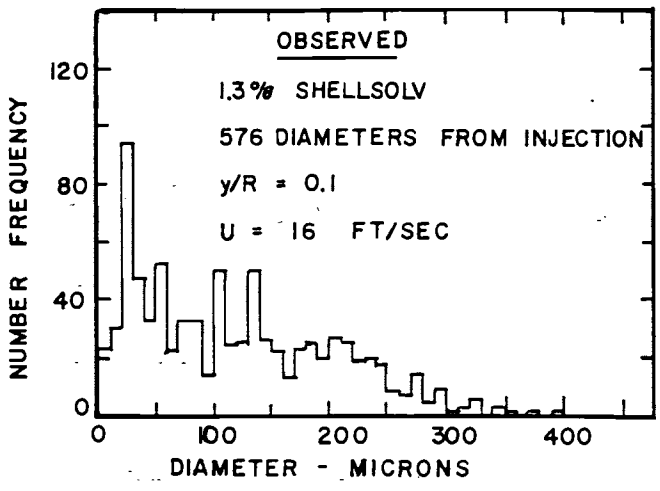

Figure 3:
Drop Size Distribution of Shellsolv in Water (Taken from AIChE Journal 1970, Vol. 16, p. 1079)

the result of the experiment under different conditions. Computer simulation has also been used as a substitute for experiments of extreme conditions which are impossible or dangerous to be carried out in a laboratory.

One of the methods of computer simulation is the Monte Carlo method which is also called the method of statistical trials. The method solves a problem by constructing a random process whose parameters are equal to those in the original problem. The variable of interest is then solved by the observing the random process.

The earliest example of Monte Carlo computation is the description of the calculation of the quantity π by Buffon (1777) using the "needle-tossing" experiment. Volser in

1850 performed the "needle-tossing" experiment and found the value of π to be 3.1596.

Sometimes the accurate modeling of a random physical process is difficult. A simplified artificial process which approximates the original process and which can be modeled by a computer may be used instead. This simplification is often necessary because of two reasons: the complete knowledge of the original process is unavailable and the computer is unable to perform complex process calculations in a reasonable time.

The Monte Carlo method has been used successfully in solving problems which are random in nature. Examples of some of these problems are found in neutron physics and detection of signals on a phone with random noise. The Monte Carlo method has also been used successfully to solve deterministic problems such as boundary-value problems and linear algebraic equations.

Accuracy of the Monte Carlo Method

The error of the Monte Carlo method, δ, can be calculated as follows:

$$\left|\frac{L}{N} - p\right| < \delta \qquad \text{(II-7)}$$

where p is the probability that event A occurs, N is the number of trials, and L is the number of trials in which event A occurs. The error is found to be of the order

$$\delta \sim \frac{1}{\sqrt{N}} . \qquad \text{(II-8)}$$

Equation (II-8) shows that a large increase in the number of tests is required in order to significantly reduce the error. In a practical problem, the error in the Monte Carlo method is of order 0.01 to 0.001 (Shreider, 1966).

Chapter III

MODEL DEVELOPMENT

The review of Sambasivam's stochastic model (1992) and the revision to his model are given in this chapter. This chapter also describes the physical system of the annular flow in gas wells and the assumptions used in the model. The chapter then describes the development of the probability function of droplet breakup in detail.

Annular Flow in Gas Wells

The flow regime under consideration in this model is the annular flow which often exists in gas wells. Other flow regimes such as slug or bubbly flow are less often encountered in gas wells, and in general these types of flow regimes are more difficult to study. Therefore, they have not been considered in this model.

A schematic diagram of annular flow in a gas well is shown in Figure 4. The gas phase flows upward in the core of the tube. The liquid film flows upward on the tube wall. The liquid film consists of oil and water condensate. Due to the immicibility of oil and water and the turbulence in the liquid film, oil and water in the liquid film are

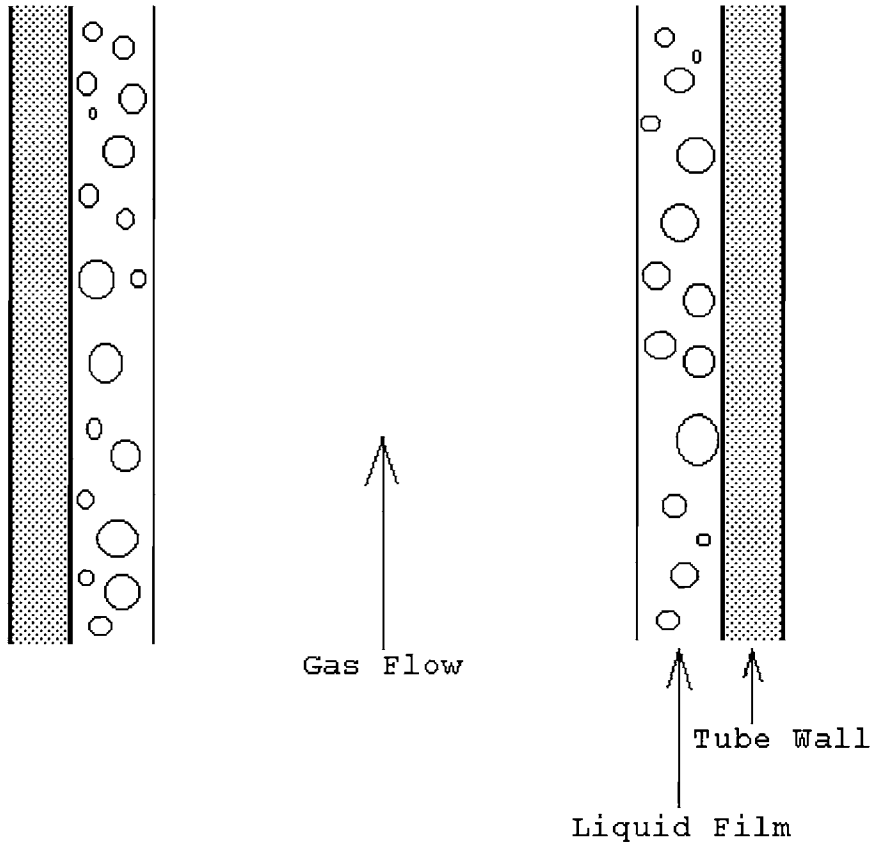

Figure 4:

Schematic Diagram of an Annular Flow

present as an emulsion. The emulsion can be either water-in-oil or oil-in-water.

At some point in a gas well, phase inversion may occur. Near the bottom of the gas well, water is usually present in a small amount in the liquid film, therefore, water is usually dispersed in oil. Due to temperature drop, the amount of water condensate in the film increases in the upper part of the well. At some point in the gas well, the amount of water in the liquid film reaches a critical value and water inverts to become the continuous phase and wets the tube wall. Corrosion is assumed to begin at the location where the phase inversion occurs.

Assumptions

Several assumptions were made about the physical system of the annular flow:

1. The liquid film on the tube wall is thin compared to the diameter of the tube. For gas wells, this assumption is justified because the liquid condensate production is usually very small compared to the gas production. For thin liquid film, all droplets in the emulsion are approximately at the same distance from the tube wall. Consequently, the breakup of droplets in the liquid film is independent of their distances from the wall.
2. The droplets in the liquid film are spherical. In reality, the droplets in the liquid film may be non-spherical.

3. Two droplets coalesce when the distance between their centers is less than $0.3(d_1 + d_2)$, where d_1 and d_2 are the diameters of the droplets.

4. No emulsifier is present in the liquid film.

5. The following properties are known:
   - temperature and pressure,
   - viscosity and density of oil and water in the liquid film,
   - velocity and thickness of the liquid film, and
   - volume fraction of water in the liquid film.

Scheme of the Simulation

The droplet coalescence and breakup in the liquid film are modeled as stochastic processes. The use of a stochastic method to model droplet coalescence and breakup in the liquid film is appropriate due to the inherent randomness of these processes in the turbulent and chaotic flow which exists in gas wells.

Figure 5 shows the algorithm used to predict phase inversion. For given flow conditions in a gas well, the stochastic process simulation predicts the stable emulsion type of the liquid film. First, the simulation produces the equilibrium drop-size distribution for both w/o and o/w emulsion. Then from the drop size distributions, the energy of w/o and o/w emulsions is calculated and compared. The emulsion with a lower energy is taken as the stable and favored emulsion. The simulation begins with a small volume

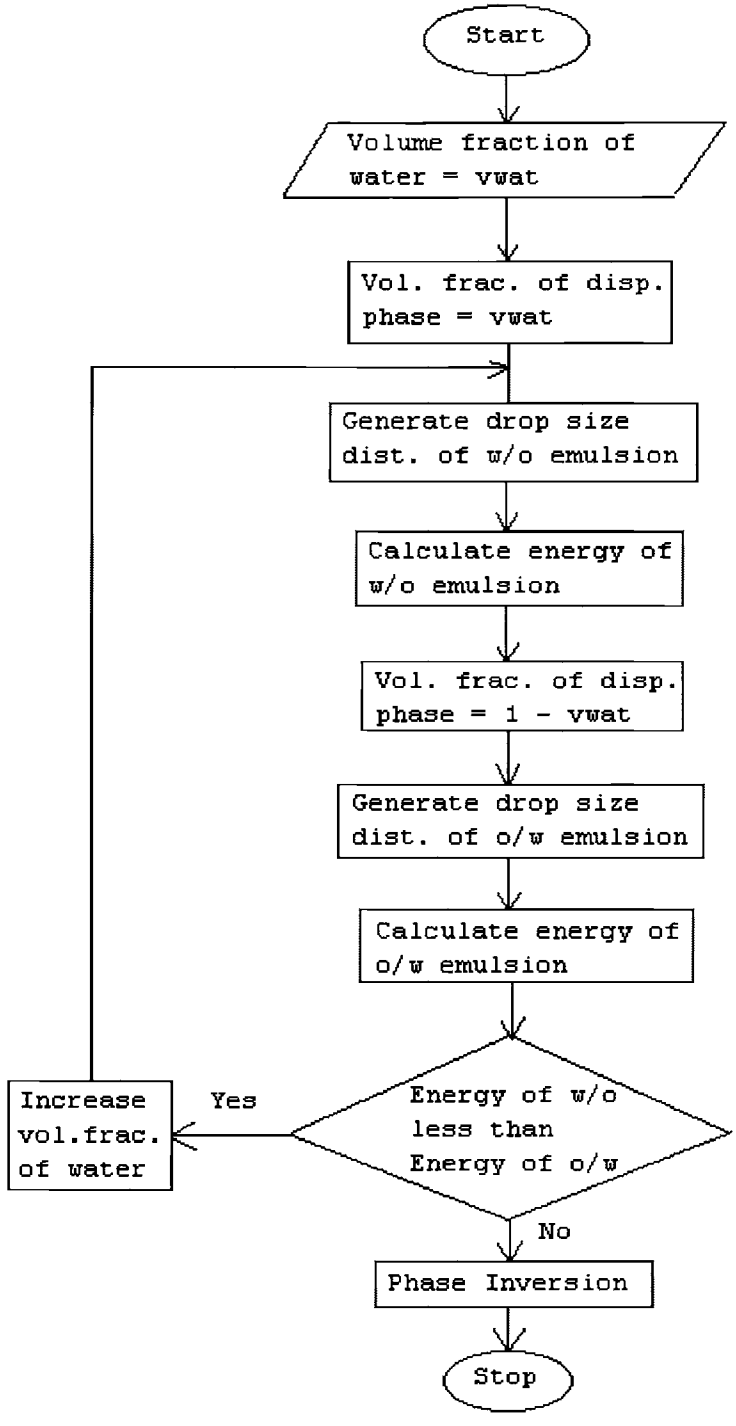

Figure 5:
Algorithm for Predicting Phase Inversion

fraction of water. The volume fraction of water is then increased and the simulation is repeated until the stability of the emulsion shifts from w/o to o/w. The simulation predicts the volume fraction of water at which the phase inversion occurs.

Start of the Simulation

In the beginning of the simulation 6084 water or oil droplets are placed in a lattice. The droplets are arranged in a face cubic center configuration. All the droplets have the same initial diameter which is equal to 30% of the maximum diameter.

The volume of the lattice depends on the volume fraction of the phases in the emulsion. The volume of the lattice is calculated as follows:

$$V_{lattice} = \frac{6084 \times 1/6\pi \; d_{ini}^{\;3}}{\phi} \qquad \text{(III-1)}$$

where d_{ini} is the initial diameter of the droplets in the lattice and ϕ is the volume fraction of the dispersed phase.

Movement of the Droplets

One droplet is chosen at random. The droplet is then moved in a random direction within the lattice. The new position of the droplet is calculated as follows:

$$X_{new} = X_{old} + (2.0\varepsilon_1 - 1.0)\delta \qquad \text{(III-2)}$$

$$Y_{new} = Y_{old} + (2.0\varepsilon_2 - 1.0)\delta \qquad \text{(III-3)}$$

$$Z_{new} = Z_{old} + (2.0\varepsilon_3 - 1.0)\delta \qquad \text{(III-4)}$$

where X_{new}, Y_{new}, and Z_{new} are the new x, y, and z coordinate of the droplet. X_{old}, Y_{old}, and Z_{old} are the initial x, y, and z coordinate of the droplet. ε_1, ε_2, and ε_3 are random numbers between zero and one. δ is the maximum allowable displacement of the droplet inside the lattice. In our model, δ is set to 10% of the maximum diameter. The terms in the brackets in the above equations allows droplets to move in the positive and negative direction. If the new position of the droplet is outside the lattice, the droplet is moved back into the lattice in a manner shown in Figure 6.

Droplet Coalescence

After the droplet is randomly moved, the possibility of the droplet coalescence is checked. Two droplets are assumed to coalesce if the distance between the centers of the droplets is less than a critical distance (d_{crit}). In our model, the critical distance is set to 0.3 (d_1 + d_2). The schematic diagram of the critical distance between two droplets is given in Figure 7.

Two droplets that coalesce will form a single droplet with diameter equal to:

$$d_{combine} = (d_1^3 + d_2^3)^{1/3} \qquad \text{(III-5)}$$

where d_1 and d_2 are the diameters of the coalescing droplets.

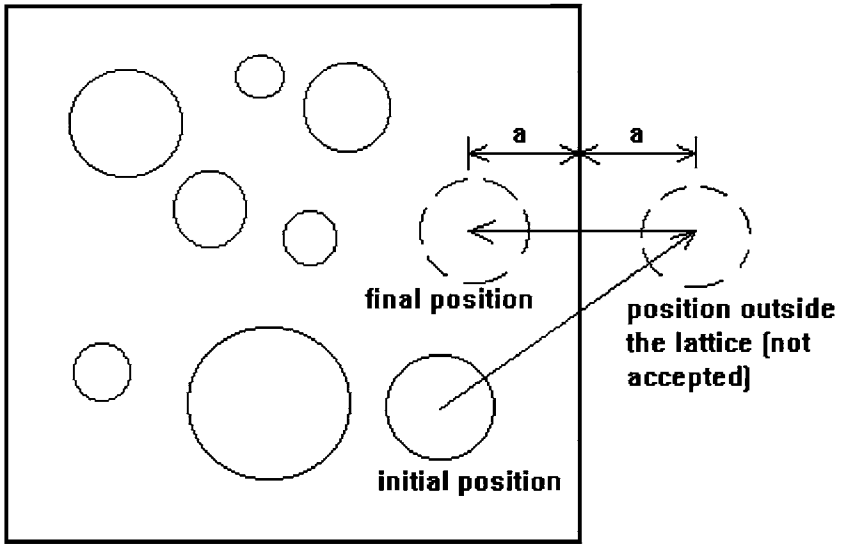

Figure 6:
Schematic Diagram of Unacceptable Droplet Movement

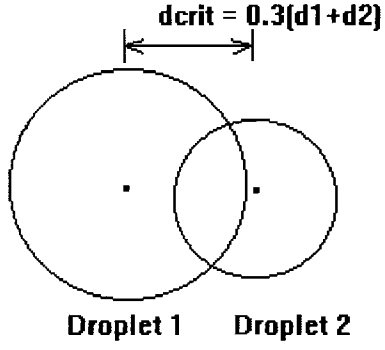

Figure 7:
Schematic Diagram of the Critical Distance

Probability of Droplet Coalescence

The probability of droplet coalescence depends on the volume fraction of the dispersed phase. A droplet is more likely to coalesce with another droplet if the volume fraction of the dispersed phase is high. On the other hand, when the volume fraction of the dispersed phase is low, a large space exists between droplets and thus reduces the probability of coalescence.

Probability of Droplet Breakup

The droplet breakup in the model can be described as follows. After the random droplet movement, another droplet is chosen randomly and its probability of droplet breakup is calculated and compared with a random number. If the probability of breakup is higher than the random number, the droplet is allowed to breakup into two equal droplets. Otherwise, the droplet does not breakup.

The probability of droplet breakup in turbulent flow depends on several factors. The computer model developed in this project accounts for the effects of droplet size, flow conditions, and viscosities. The probability of breakup is given as follows:

$$p = 0.5(p_1 + p_2) \qquad \text{(III-6)}$$

where p_1 accounts for the effect of droplet size and flow conditions and p_2 accounts for the effect of viscosity. 0.5 is a normalizing factor.

1. Droplet Size and Flow Conditions

The size of a droplet affects the probability of the droplet breakup. Hinze (1955) and Sleicher (1962) used the term *maximum diameter* (d_{max}) to define the largest stable drop size that can exist in a given flow. The closer the diameter of the droplet to d_{max}, the greater the probability for the droplet to breakup. In our model, the term *minimum diameter* (d_{min}) is used to define the smallest drop size that can exist in a given flow. The w/o and o/w emulsions in the gas well are assumed to have a drop size distribution between d_{min} and d_{max}. D_{min} can be estimated by using equation II-6. D_{max} can be estimated by using equation II-4 or II-5.

A linear relationship of droplet size to the probability of droplet breakup is used in our model. The relationship is similar to the model used by Collins and Knudsen (1977). However, a constant, k, is present in our model to take into account the flow conditions in the gas well. The equation is given as follows:

$$p_1 = k\frac{(d - d_{\min})}{(d_{\max} - d_{\min})}. \qquad \text{(III-7)}$$

The greater the turbulence in the liquid film, the larger the value of k is. The constant, k, can have a value from zero to one. The turbulence in the liquid film is indicated by the Reynolds number. In this model the relationship of the constant k and the Reynolds number is proposed as follows:

$$k = \exp\left(\frac{-1000}{\mathrm{Re}_l}\right) \qquad \text{(III-8)}$$

where Re_l is the Reynolds number of the liquid film. The constant, 1000, is to give k a value of 0.62 when Re_l is 2100. The exponential form of equation III-8 limits the value of k from 0 to 1.

The Reynolds number in equation III-8 is defined as follows:

$$\mathrm{Re}_l = \frac{2\rho_l V \delta}{\mu_l} \qquad \text{(III-9)}$$

where ρ_l is the density of the liquid film. V is the average velocity of the liquid film. δ is the thickness of the liquid film. μ_l is the viscosity of the liquid film.

2. Viscosity Ratio

Viscosity ratio of the dispersed to the continuous phase is a very important factor in droplet breakup. Viscosity is a measure of resistance to deformation. A material with high viscosity requires a greater energy to deform. Stone (1994) argued that the viscosity ratio of the dispersed phase to the continuous phase (μ_d/μ_c) was the most important variable in determining droplet breakup. If μ_d/μ_c was of order of magnitude greater than one, the internal flow processes of droplets in an emulsion were damped, resulting in less frequent droplet breakup. The condition resulted in a drop size distribution with a small number of uniformly size drops. When μ_d/μ_c is low (i.e. 0.01), Stone

observed that droplets broke readily, resulting in a drop size distribution with many small droplets.

Sambasivam (1992) in the study of phase inversion also concluded that viscosity played an important factor in droplet breakup. When the viscosity of the dispersed and the continuous phase was not taken into account in droplet breakup, Sambasivam's model always predicted phase inversion at 50% volume fraction of the dispersed phase.

All studies in droplet breakup conclude that an increase in droplet viscosity results in an increase of the energy needed to break the droplet. The reason is that an additional energy is needed to overcome the internal viscous dissipation. Based on the above observations, the following relationship of the viscosity ratio to the droplet breakup is proposed:

$$p_2 = \exp\left(\frac{-\mu_d}{\mu_c}\right) \qquad \text{(III-10)}$$

The probability of droplet breakup approaches one as μ_d/μ_c approaches zero. As μ_d/μ_c becomes large, the probability approaches zero.

Accepting and Rejecting Droplet Movement

In the simulation, droplet movement which causes the system energy to decrease or remain unchanged is always accepted. When a droplet coalesces with another droplet, they form a single droplet with a lower surface area and thus lowers the system energy. When droplet movement does

not result in coalescence, the system energy remains constant.

Droplet movement which causes the system energy to increase is only accepted on certain conditions. When a droplet breaks into two equal droplets the surface area and thus system energy increases. The droplet is allowed to break only if its probability of breakup is higher than a random number. Otherwise, the droplet breakup is rejected.

Chapter IV

RESULTS AND DISCUSSION

Prediction of Drop Size Distribution

Since the drop size distribution of an emulsion determines its surface energy, a good prediction of drop size distribution is required in the model in order to predict the stability of the emulsion. The ability of the model to predict the drop size distribution was tested against two limiting cases. In both cases, the simulations were started with the initial diameter of 5.463 micron.

Case I was a hypothetical case in which all droplets in the emulsion had a zero probability of breakup. The result of the simulation is shown in Figure 8. The droplets in Case I were found to have a uniform size close to the maximum diameter.

The result of the simulation for Case I agrees with our expectation. If droplets in an emulsion can only undergo coalescence, eventually all the droplets will coalesce to form the droplets with the maximum allowable size.

The second case tested was a hypothetical case in which all droplets had a probability of breakup equal to one. The

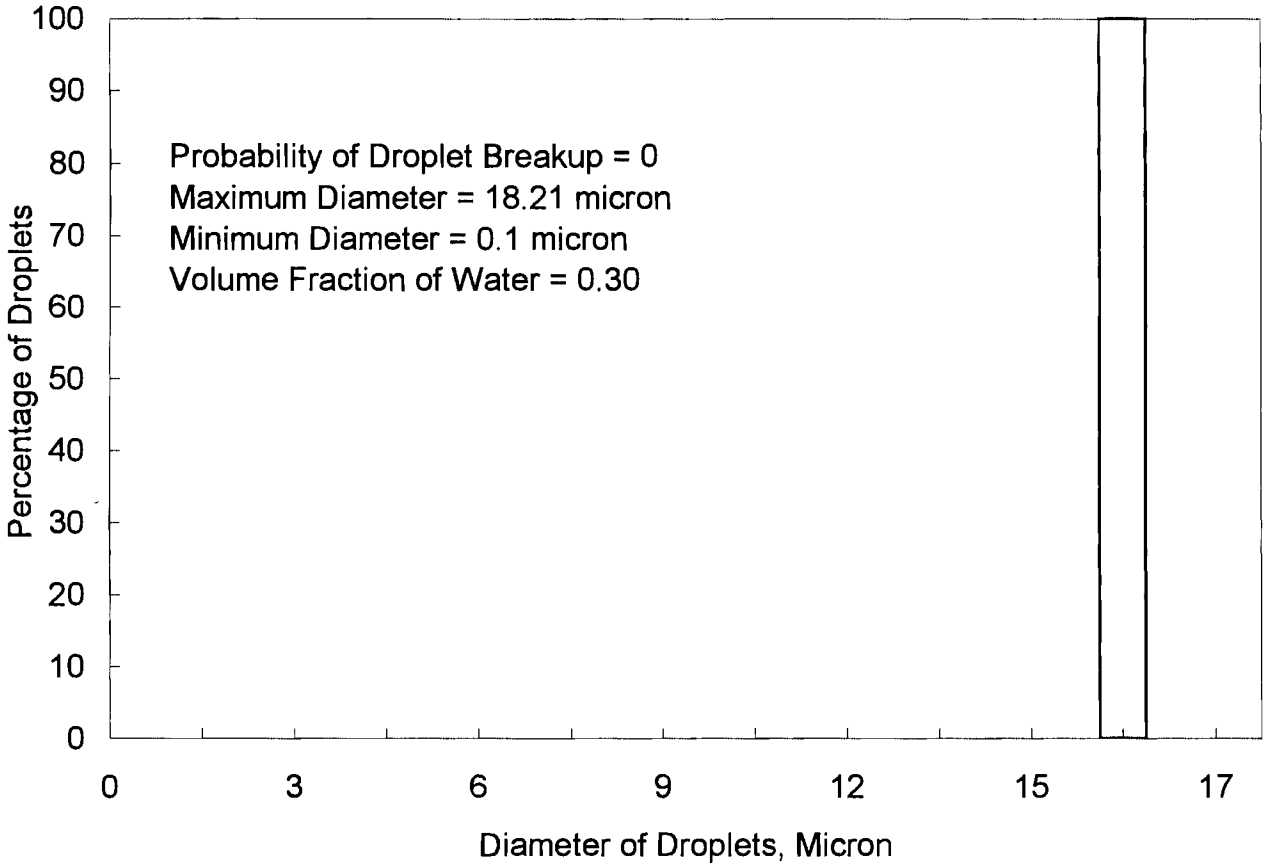

Figure 8:
Drop Size Distribution for Case I
(Probability of Droplet Breakup = 0)

result of the simulation is shown in Figure 9. The majority of the droplets in Case II were found to have drop sizes close to the minimum diameter. The tail of the distribution was the result of droplet coalescence that existed in the system. Even though the tail of the distribution accounted for only 20% of the total number of droplets, it accounted for about 90% of the total volume in the system. The droplets in Case II were log-normally distributed. The maximum of the distribution was skewed to the minimum diameter.

Again, the result of the simulation was as expected. In Case II, droplet breakup was a more dominant process than droplet coalescence. Since each of the droplets in the emulsion underwent droplet breakup more often than coalescence, eventually they formed droplets with smaller diameters.

Evolution of the System Energy

The evolution of the system energy for Case I and II as a function of the number of Monte Carlo moves are given in Figures 10 and 11. For Case I where no droplet breakup existed, all the droplets coalesced to reduce their surface areas and formed a more stable system. The system reached equilibrium at about 100,000 moves. At the equilibrium, the droplets stopped coalescing because the large space in between them made coalescence difficult. The evidence is

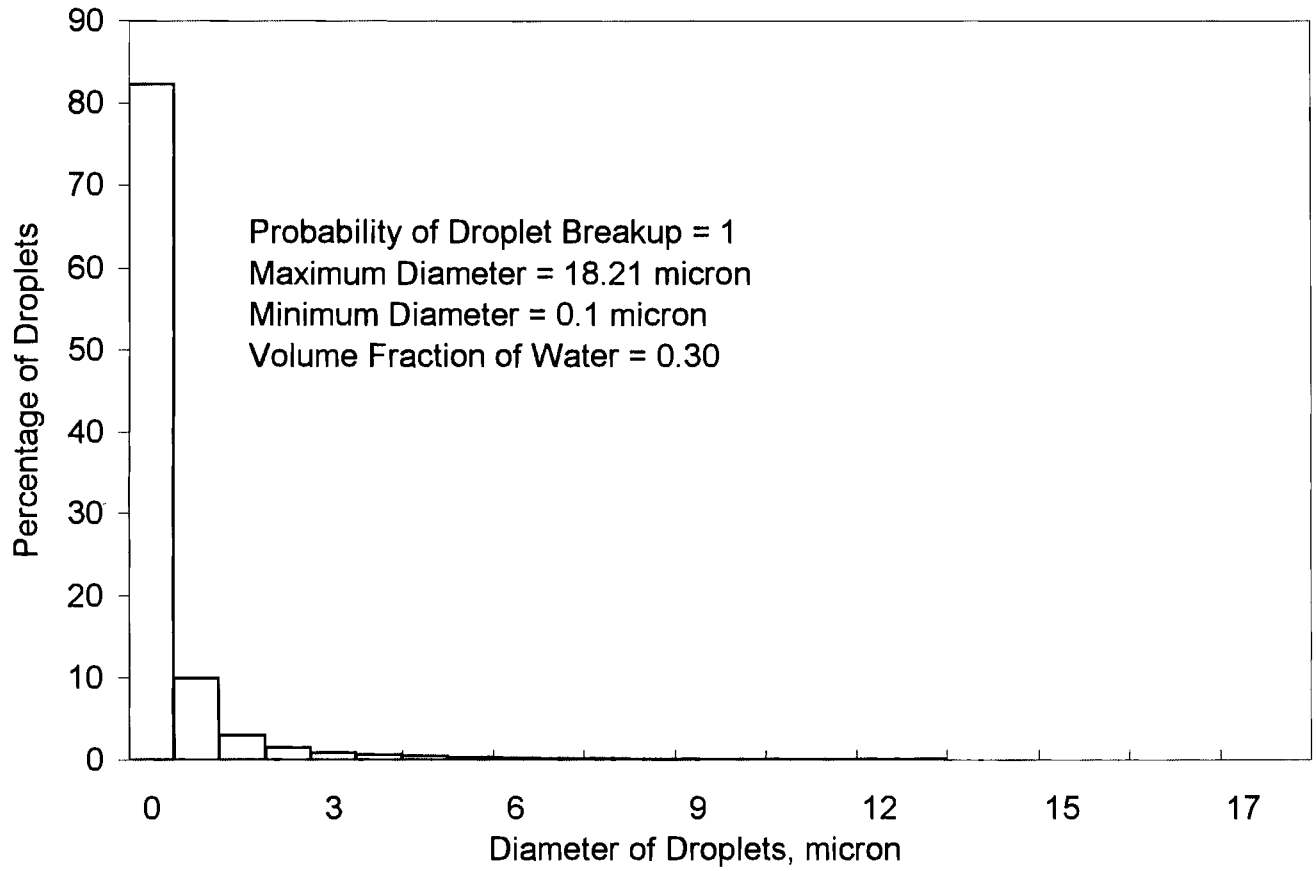

Figure 9:
Drop Size Distribution for Case II
(Probability of Droplet Breakup = 1)

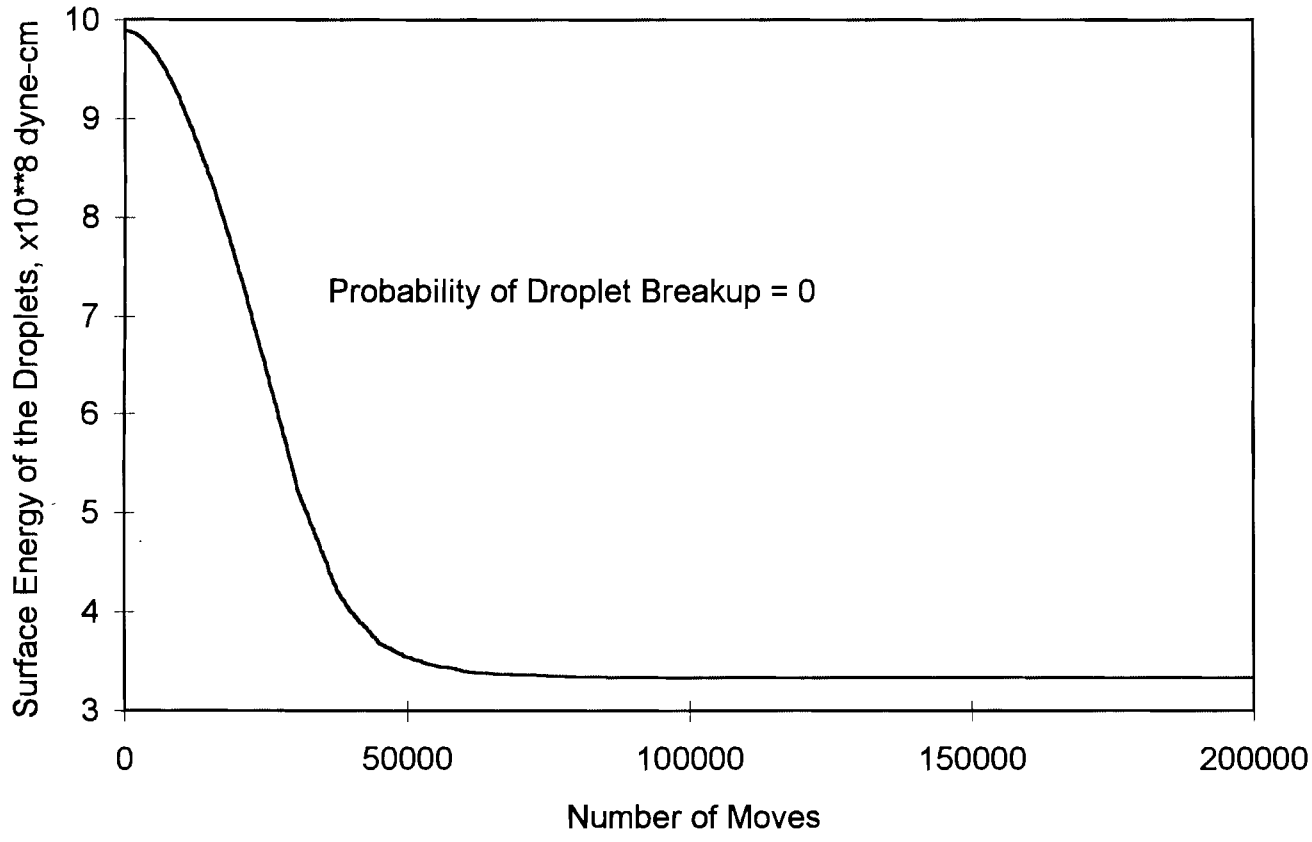

Figure 10:
Energy of Droplets in Case I as a Function of the Number of Droplet Moves

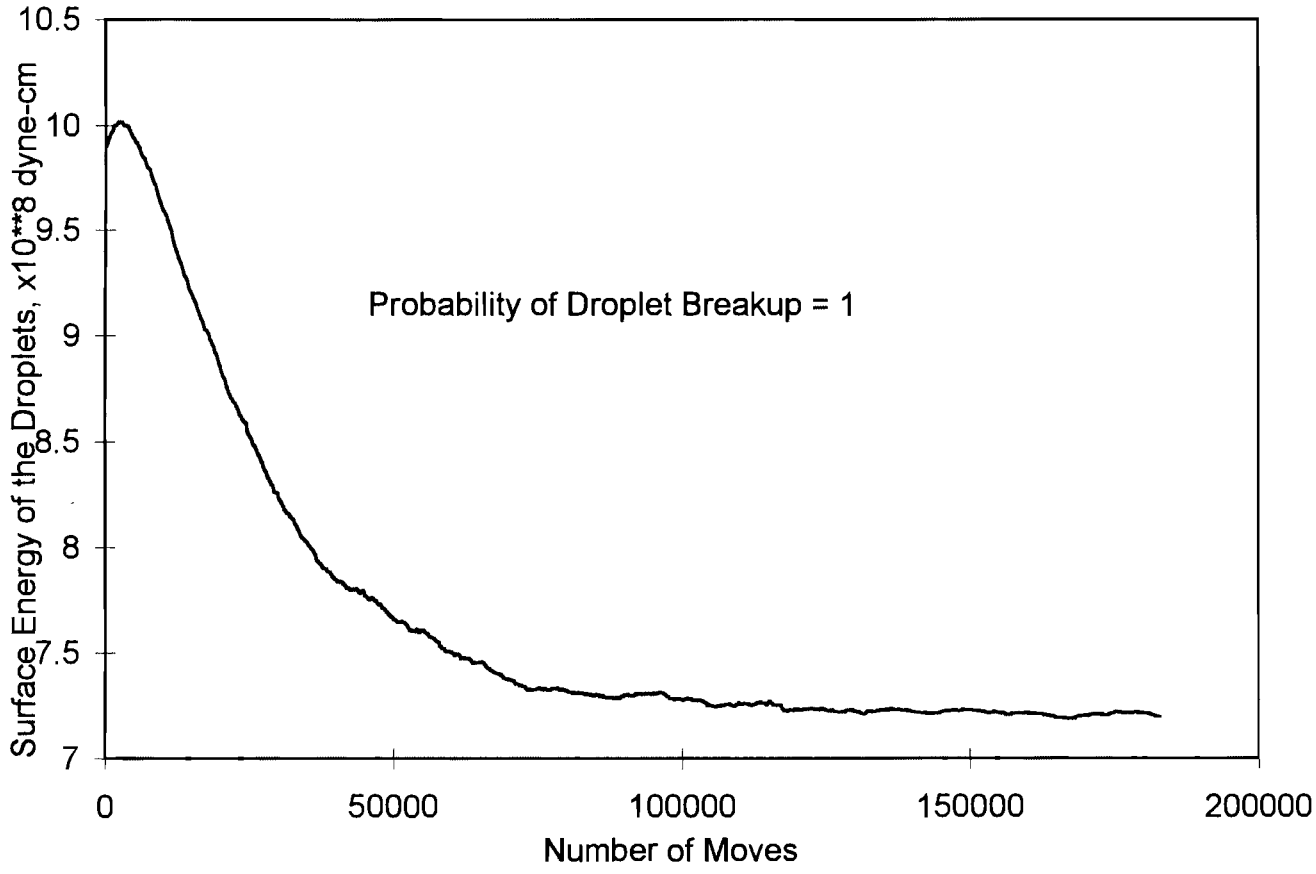

Figure 11:
Energy of Droplets in Case II as a Function of the Number of Droplet Moves

from the number of droplets that had been greatly reduced from 6084 to 234 at the equilibrium.

For Case II, droplet breakup was more dominant than droplet coalescence. More surface areas were created at the beginning; hence a small rise in the energy of the system occurred. As the simulation progressed, the frequency of droplet coalescence increased. More and more droplets with diameters greater than the initial diameter were formed. The energy of the system started to decrease and eventually reached an equilibrium after 200,000 moves.

The evolution of energy in Case II at first seemed to contradict with ones expectation. Since the simulation produced many droplets (about 95%) with diameter less than the initial diameter, one would expect the surface areas and thus the energy of the system to increase instead of decreasing. However, the effect of droplets with diameter greater than the initial diameter could not be underestimated.

Eventhough the droplets with diameters greater than the initial diameter (5.463 micron) accounted for only 5% of the total droplet population, they actually accounted for about 50% of the total droplet volume. These droplets reduced the surface areas greatly and counteracted the effect of the smaller droplets. In Case II, the droplets with diameters greater than the initial diameter were found to have a greater effect in reducing the surface areas than the smaller droplets in increasing the surface areas.

Therefore, the energy of the system decreased as shown in Figure 11.

The model predicted drop size distribution as expected for the hypothetical Case I and II. In Case I and II, the probability of droplet breakup was set to be zero and one, respectively, for all the droplets in the system. For a general case, the droplet breakup in the model is dependent on the size of the droplet, the viscosity ratio of the dispersed and continuous phase, and the turbulence in the liquid phase.

Comparison of Simulated Drop Size Distributions with Experimental Data

For general cases, comparisons of simulated drop size distributions with experimental data are desirable. Unfortunately, no drop size distribution data in a vertical-annular flow has been reported in the literature. Therefore, comparisons were made with systems other than the vertical-annular flow.

A comparison was made (Case III) with the drop size distribution obtained by Schwarz and Bezemer (1956) which is shown in Figure 12. The emulsion was prepared from water and crude oil. Other data such as the viscosities and Reynolds number were not specified. Therefore, the input data for the simulation had to be estimated. Several simulations with different input variables were performed. The simulation produced a drop size distribution in good

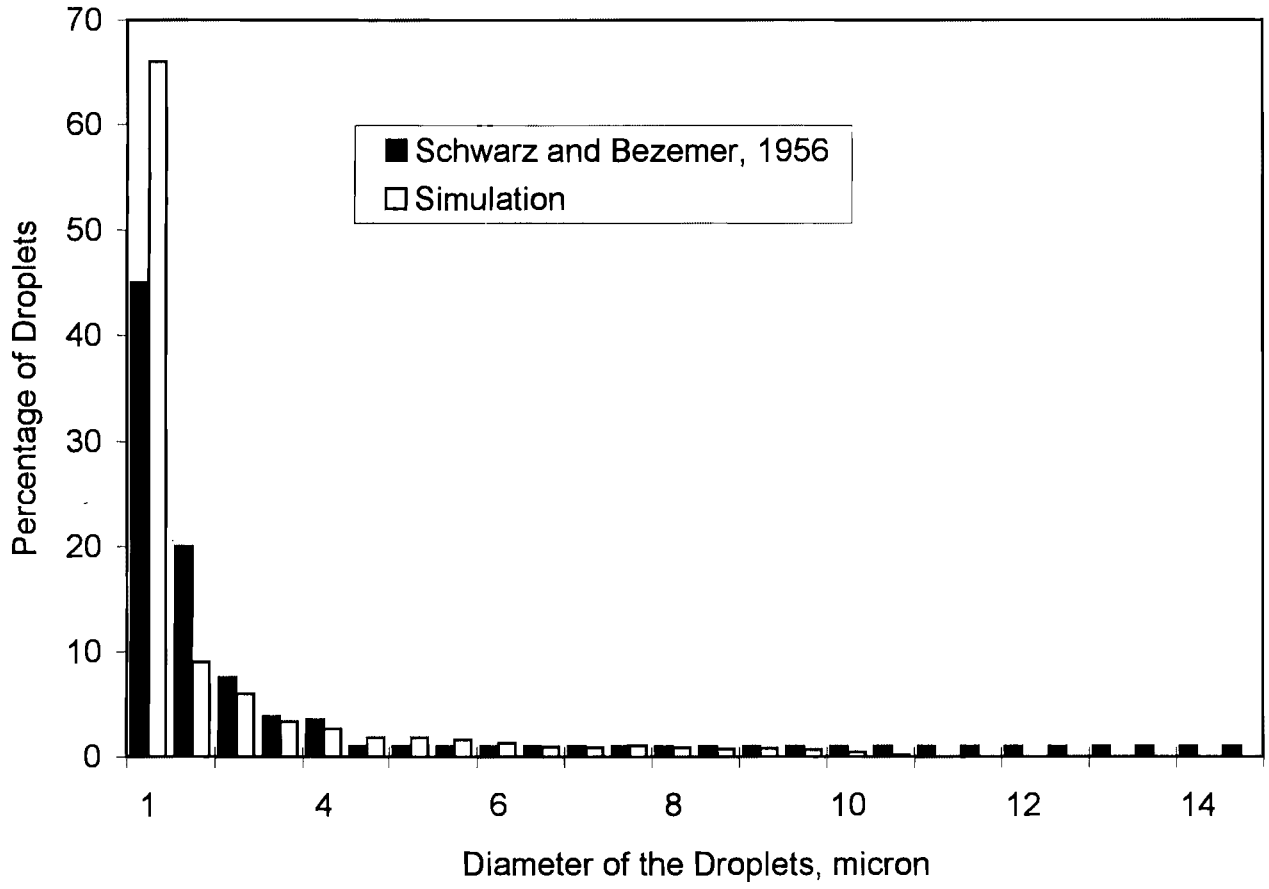

Figure 12:
Comparison of Experimentally Obtained and Simulated Drop Size Distribution of Water in Crude Oil

agreement with the experimental data when the following input data were used: the viscosities of the water and oil equal to 1.0 cP, the Reynolds number equal to 2000, the volume fraction of the water equal to 0.30.

The simulated drop size distribution which is also given in Figure 12 compared favorably with the data obtained by Schwarz and Bezemer (1956). Both drop size distributions show that about 70% of the droplets have diameters less than 2 micron. Both distributions also show that only a small fraction of droplets have diameter in the range of 5 to 15 micron.

Another comparison was made (Case IV) with the drop size distribution obtained by Sibree (1933) using a Hurrell mill. The Hurrell mill consists of a casing in which a rotor composed of two discs shaped in section like a truncated cone revolves in close proximity to a similarly shaped stator ring. The emulsion was made from a viscous paraffin dispersed in 1% sodium oleate solution. The sodium oleate acted as an emulsifier. The volume fraction of the dispersed phase was 0.50. The viscosity of the dispersed and continuous phase, as well as the Reynolds number of the liquid, was not specified in the data. Thus, the input data to the simulation had to be estimated. Again, several simulations with different input variables were performed. The simulation produced a drop size distribution in closest agreement with the experimental data when the viscosity ratio of the dispersed to the continuous phase was set to

one, the Reynolds number was set to 10000, and the maximum and the minimum diameters of the droplets were set to 18.21 and 1.0 micron, respectively.

The simulated drop size distribution did not compare favorably with Sibree's data. The difference of the drop size distribution produced by the simulation and that obtained from the experiment could be accounted for. The drop size distribution from Sibree's data is given in Figure 13. The simulated drop size distribution from the model is shown in Figure 14. The difference in the two distributions was that droplets with diameter greater than 6 micron was present only in a very small fraction in the distribution obtained by Sibree. The difference could be explained as follows. Since the emulsion used by Sibree contained an emulsifier, droplet coalescence was very small or non-existent in the emulsion. Therefore, the formation of bigger droplets in the emulsion was not favored. In contrast, our model which produced drop size distribution in Figure 14 did not account for the presence of the emulsifier. Therefore, droplet coalescence which formed larger droplets were allowed in our model.

Conservation of Mass in the Simulation

The mass of the system was always conserved in the simulations. The mass was calculated at the beginning and at the end of the simulations. Only small truncation errors

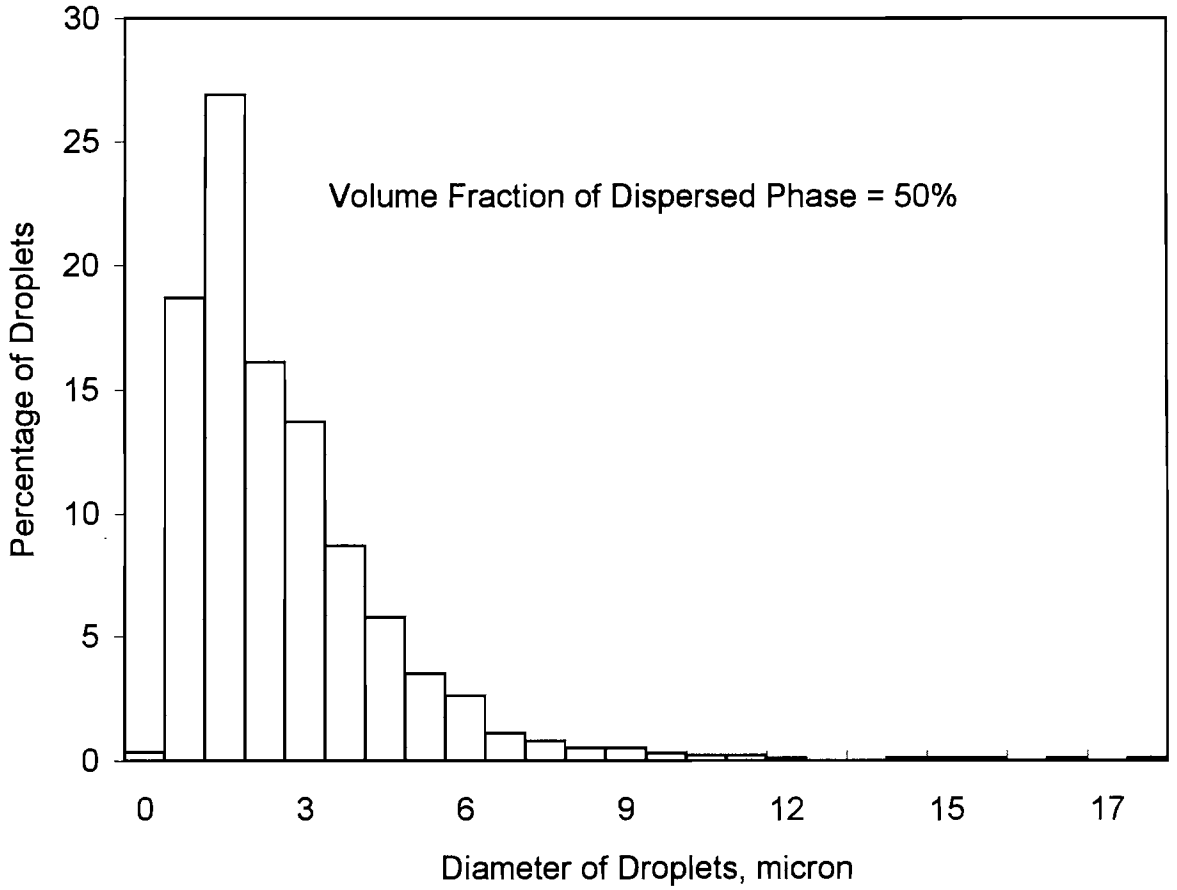

Figure 13:
Drop Size Distribution of Viscous Paraffin in 1% Na Oleate Solution
(Sibree, 1933)

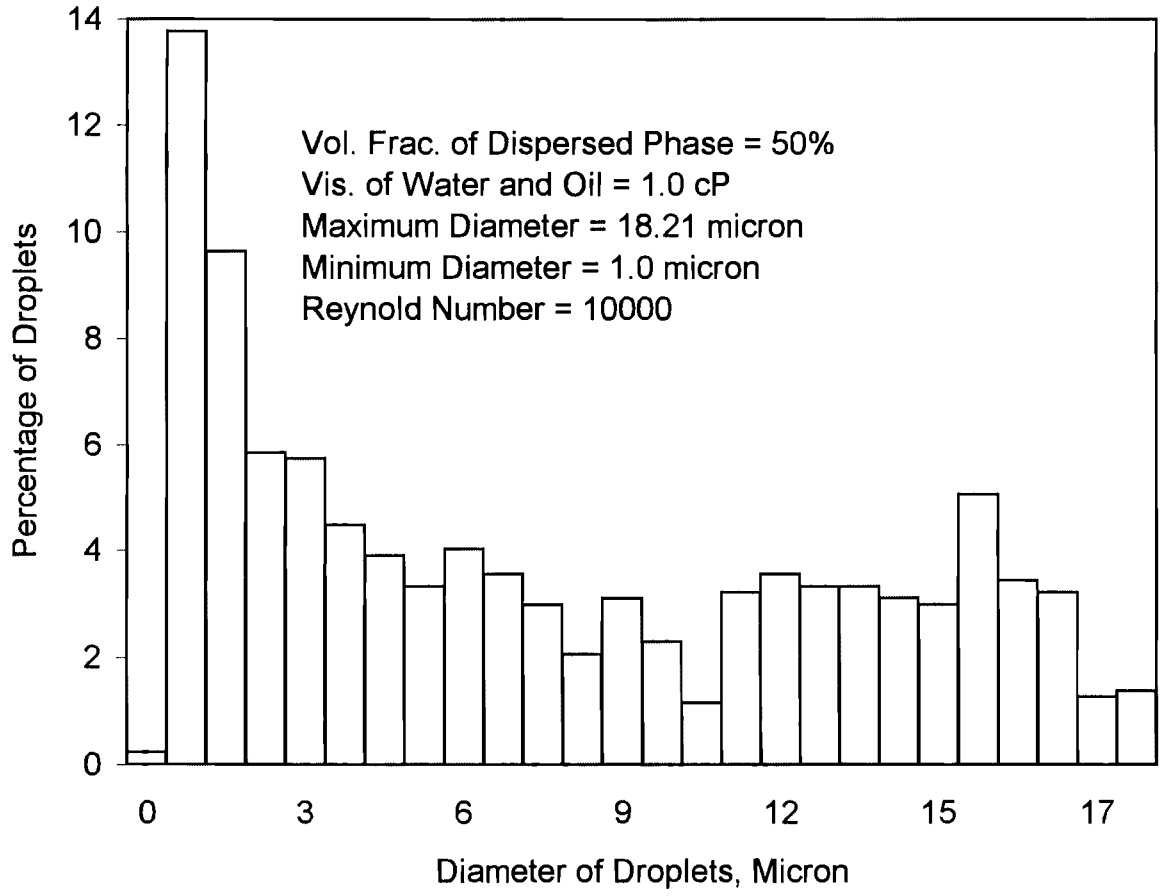

Figure 14:
Simulated Drop Size Distribution of Viscous Paraffin in 1% Na Oleate Solution

were observed in all cases. The truncation errors for Case I, II, III, and IV are given in Table I.

Table I

Truncation Error in the Simulations

Case No.	# of Moves	% Error
I	200,000	0.089
II	200,000	0.015
III	100,000	0.0009
IV	200,000	0.010

Prediction of the Phase Inversion

To predict the volume fraction of water at which the w/o emulsion inverts to o/w emulsion, simulations were performed for both types of emulsions at different volume fractions of water. Simulations are usually started with a lower volume fraction of water. If w/o emulsion is more stable than o/w emulsion for a given volume fraction of water, the volume fraction of water is increased and simulation is repeated. Phase inversion occurs when o/w emulsion has a lower surface energy than w/o emulsion.

A typical run is shown in Figure 15. The viscosity of water and oil were 1.0 and 2.5 cP, respectively. The Reynolds number of the liquid film was 10,000. The simulations were performed with a volume fraction of water

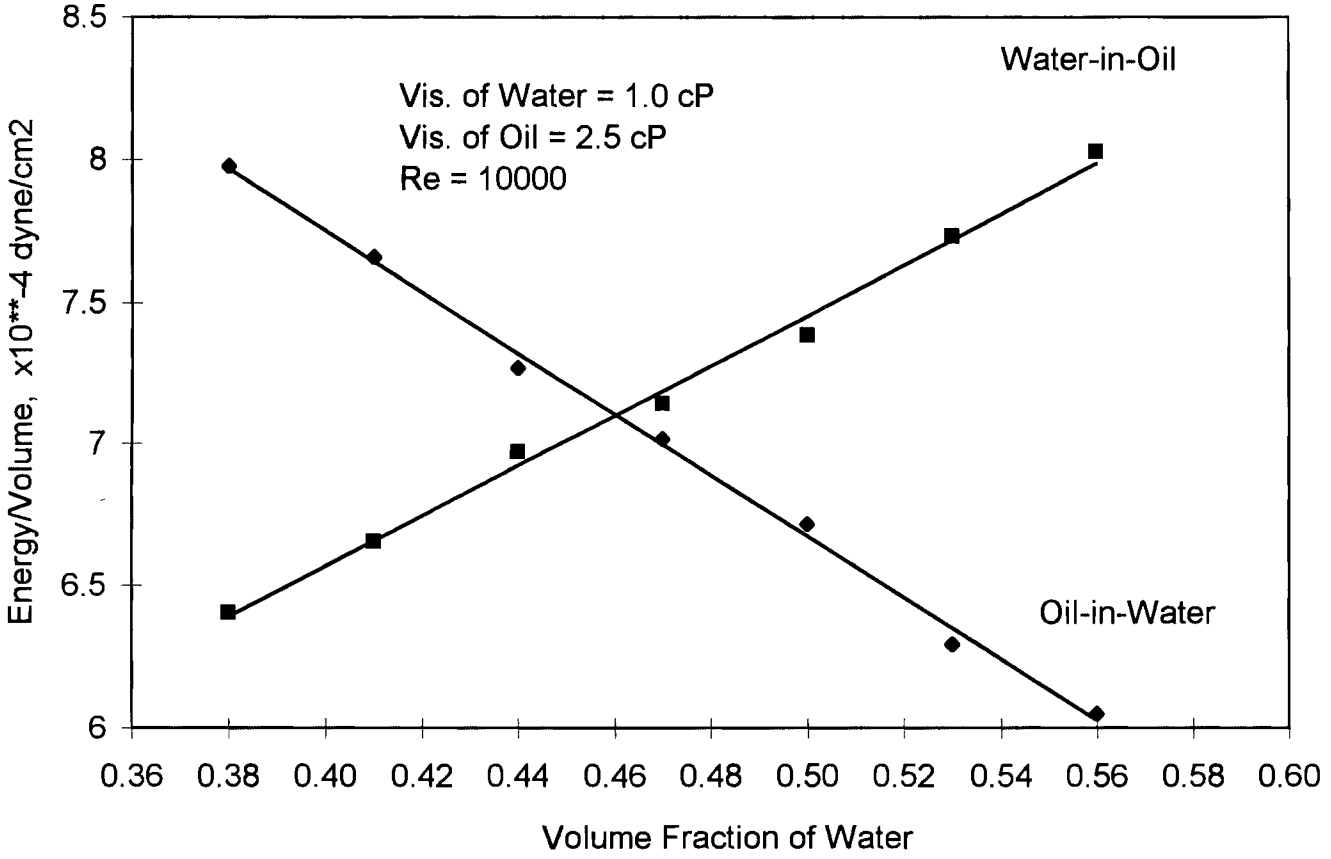

Figure 15:
Energy of Droplets in Water-in-Oil and Oil-in-Water Emulsion as a Function of the Volume Fraction of Water

ranging from 0.38 to 0.56 with an increment of 0.03. At volume fraction of water about 0.46, the o/w emulsion became more stable than that of w/o. Therefore, the model predicted that phase inversion occurred at volume fraction of water of 0.46 for the given flow conditions.

Effect of the Viscosity Ratio

To investigate the effect of the viscosity ratio on phase inversion, simulations were performed at different viscosity ratios. In these simulations, the Reynolds number of the liquid film was constant. The result of these simulations with Reynolds number of 100 is given in Figure 16. Viscosity ratios used were 0.01, 0.05, 0.4, 1.0, 2.5, 20, and 100. The result shows that as the viscosity ratio decreased, the volume fraction of water at which phase inversion occurs also decreased. Figure 16 shows that the effect of the viscosity ratio vanished when the ratio was greater than 100 or smaller than 0.01. Figure 16 also shows that as the viscosity of the oil phase increased, the oil phase became more likely to be dispersed which agrees with the observation by Clarke and Sawistowski and Selker and Sleicher (1965).

Effect of Turbulence

To investigate the effect of turbulence of the liquid film on phase inversion, simulations were performed at different Reynolds number. The results of the simulations

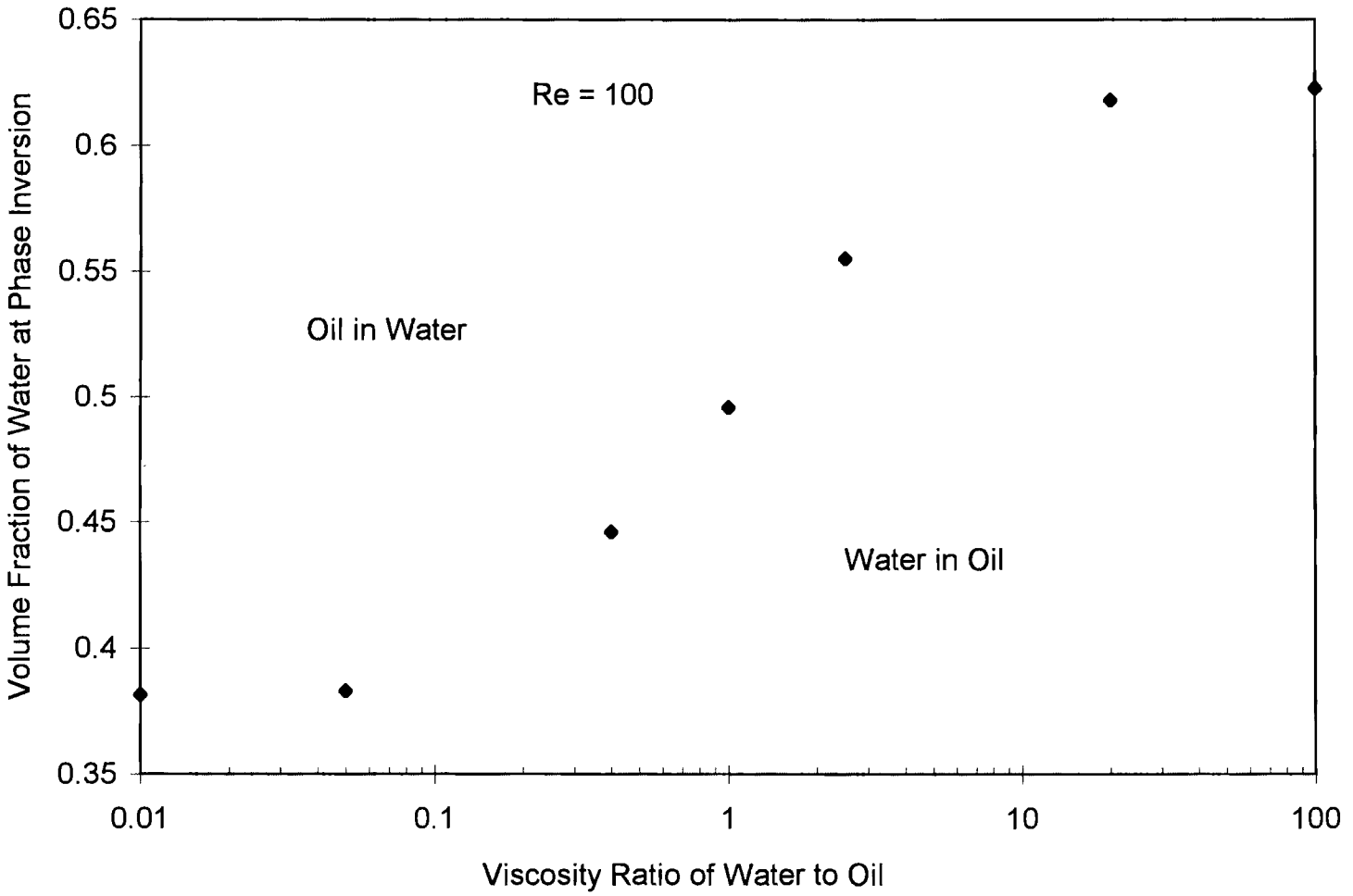

Figure 16:
Dependency of Phase Inversion on Viscosity Ratio of Water to Oil

for Reynolds number of 100, 1000, and 10000 are shown in Figure 17.

As the Reynolds number of liquid increased, the phase inversion occurred at a higher volume fraction of water if the viscosity ratio was less than one. The results in Figure 17 agree with those obtained from stirred tank experiments. Quinn and Sigloh (1963) and Selker and Sleicher (1965) found that the volume fraction of the dispersed phase at phase inversion increased as the stirrer speed (Reynolds number in the liquid phase) increased. Figure 17 also shows that when the viscosity ratio was greater than one, the phase inversion occurred at a higher volume fraction of water as the Reynolds number decreased.

Comparison of the Simulation Results on Phase Inversion with Experimental Data

One of the latest studies on phase inversion was done by Brooks and Richmond (1993). They studied phase inversion of water-in-oil emulsions to oil-in-water emulsions in a stirred tank. Oils with viscosity ranging from 0.7 to 200 cP were used to investigate the effect of viscosity on phase inversion. The stirrer speed was varied from 400 to 800 rpm in order to investigate the effect of turbulence. The results from their experiments were found to agree with the results obtained from our model.

The results of the study by Brooks and Richmond (1993) and by our model showed that when the oil viscosity

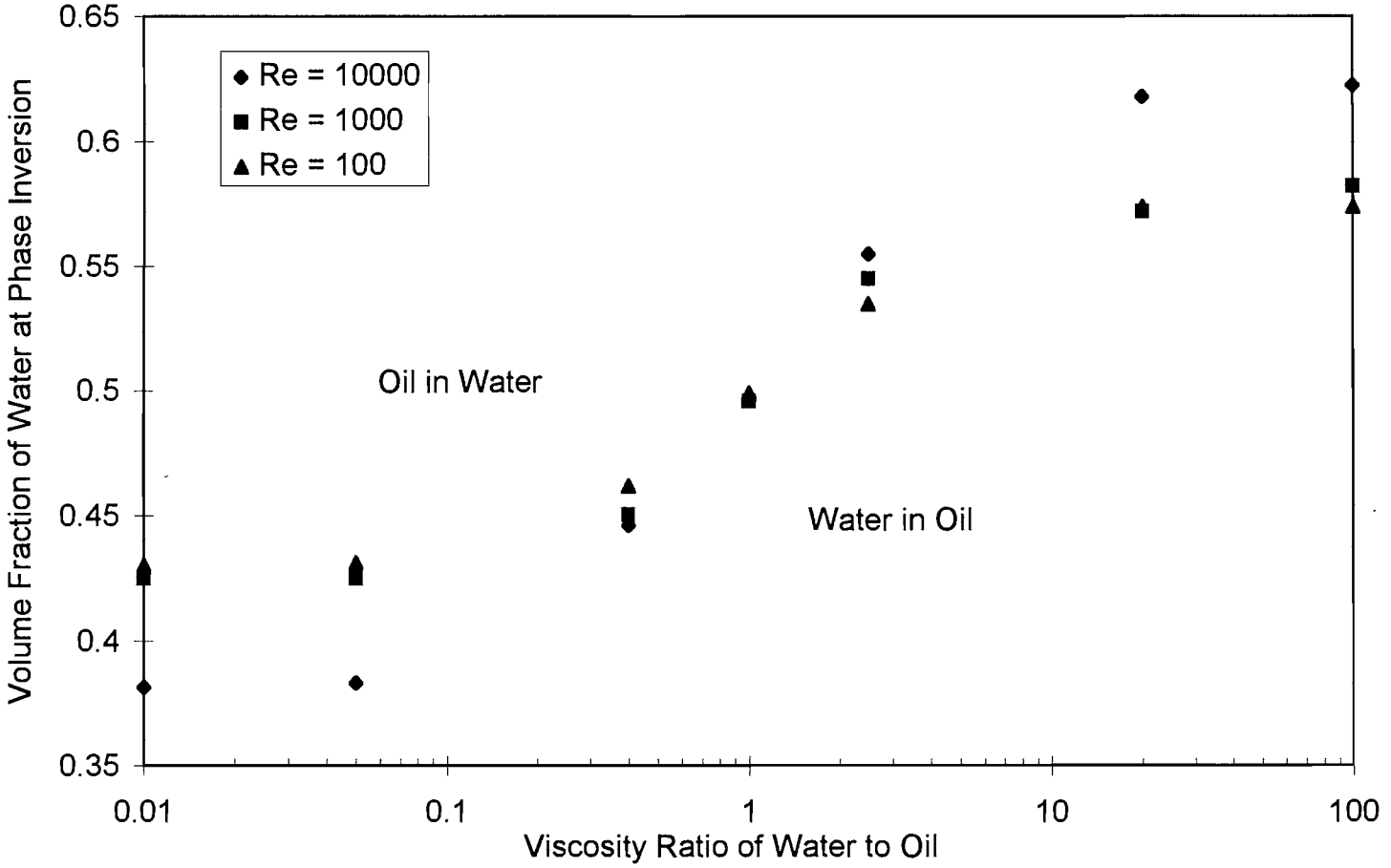

Figure 17:
Dependency of Phase Inversion on the Viscosity Ratio with Reynolds Number as a Parameter

increased, the volume fraction of water at phase inversion decreases. By increasing the oil viscosity from 0.7 cP to 200 cP, Brooks and Richmond found that the volume fraction of water decreased and reached a constant value of 0.15 when the oil viscosity was above 200 cP. The simulation results showed the same trend. The simulation predicted the volume fraction of water to remain constant at 0.38 when the oil viscosity was above 100 cP. The trend observed in both studies showed that a minimum amount of water needed to be present in w/o emulsion in order for phase inversion to occur.

Both studies also showed that when the turbulence increased, the volume fraction of water at phase inversion also increased. By increasing the stirrer speed from 400 to 800 rpm, Brooks and Richmond (1993) found that the volume fraction of water at phase inversion increased but not significantly. Simulation results showed that the effect of turbulence was only significant at low Reynolds number and high oil viscosity. At high Reynolds number, the effect of turbulence became insignificant.

CHAPTER V

CONCLUSIONS AND RECOMMENDATIONS

Conclusions

A unique model of phase inversion prediction has been developed. Given the conditions in a gas well, the model predicts the emulsion type of the liquid film on the tube wall. The model predicts the water-wet zone in gas wells and therefore predicts the location where corrosion is most likely to occur.

The phase inversion prediction from our model agrees qualitatively with the experimental results obtained by Brooks and Richmond (1993). The model and the experimental results of Brooks and Richmond (1993) agrees on the following major points:

- As the oil viscosity is increased, the volume fraction of water at phase inversion decreases and reaches a critical value when the oil viscosity reaches a certain value.
- As the turbulence in the liquid phase is increased, the volume fraction of water at phase inversion also increases.
- Turbulence in the liquid phase has a less significant effect on phase inversion than viscosity.

Recommendations

To gain more confidence in our model, a comparison with the experimental data of phase inversion in the annular flow is needed. Currently, the results from our model have not been compared with the experimental data obtained in the annular flow because no such study has been reported in the literature.

A correlation can be proposed from the simulation results and incorporated into the DREAM software. The DREAM software is a computer software developed at Oklahoma State University. The software is used to predict the corrosion rate in gas wells. The present work can be incorporated into DREAM software as follows. For any zone in a gas well, the DREAM software can be used to provide all the necessary properties needed as the input to the phase inversion simulation. The physical properties needed are the viscosity of water and oil, and the Reynolds number of the liquid phase. The correlation can then be used to determine whether a particular zone in a gas well is water-wet or oil-wet.

REFERENCES

Allen, M. P., Tildesley, D. J., *Computer Simulation of Liquids*; Oxford University Press: New York, 1987.

Bhatnagar, S. S. The Reversal of Phases by Electrolytes and the Effects of Free Fatty Acids and Alkalis on Emulsion Equilibrium. *J. Chem. Soc.* **1920**, *119*, 61.

Bradburn, J. B.; Water Production - An Index to Corrosion. *South Central NACE Meeting*, Houston, Texas, 1977.

Brooks, B. W.; Richmond, H. N. Phase Inversion in Non Ionic Surfactant-Oil-Water System-III. The Effect of the Oil-Phase Viscosity on Catastrophic Inversion and the Relationship Between the Drop Sizes Present Before and After Catastrophic Inversion. *Chem. Eng. Sci.* **1994**, *49(11)*, 1843-1853.

Choi, H. J.; Cepulis, R. L.; Lee, J. B. Carbon Dioxide Corrosion of L-80 Grade Turbular in Flowing Oil-Brine Two Phase Environments. *Corrosion* **1989**, *45*, 943-950.

Clarke, S. I.; Sawitowski, H. Phase Inversion of Stirred Liquid-Liquid Dispersions Under Mass Transfer Conditions. *Trans. Instn. Chem. Engrs.* **1978**, *56*, 50-55.

Clay, P. H. Mechanism of Emulsion Formation in Turbulent Flow. *Kononklijke Nederlandsche Akademia Van Wetenschappen* **1940**, *43*, 852-865, 978-990.

CO_2 Corrosion in Oil and Gas Production; NACE Task Group T-1-3, Eds.; National Association of Corrosion Engineers; Houston, 1984, 11-58.

Collins, S. B.; Knudsen, J. G. Drop Size Distributions Produced by Turbulent Pipe Flow of Immicible Liquids. *AIChe J.* **1970**, *16*, 1072-1080.

Crolet, J. L.; Bonis, M. R. An Optimized Procedure for Corrosion Testing Under CO_2 and H_2S Gas Pressure. *Material Performance* **1990**, *29(7)*, 81-86.

DeWaard, C.; Milliams, D. E. Carbonic Acid Corrosion of Steel. Corrosion, **1975**, 31, 177-181.

Gatzke, L. K.; Hausler, R. H. A Novel Correlation of Tubing Corrosion Rates in Deep, Hot Gas Well with Water and Gas Production Rates. *Advances in CO_2 Corrosion* **1984**, *1*, 87-102.

Hinze, J. O. Fundamentals of the Hydrodynamic Mechanism. *AIChe J.* **1955**, *1*, 289.

Ikeda, A.; Ueda, M.; Mukai, S. CO_2 Behavior of Carbon and Cr Steels. *Advances in CO_2 Corrosion* **1984**, *1*, 39-51.

Johnson, B. V.; Choi, H. J.; Green, A. S. Effects of Liquid Wall Shear Stress on CO_2 Corrosion of X-52 C-Steel in Simulated Oilfield Production Environments. *Corrosion* **1991**, Paper No. 573, Cincinnati, Ohio.

Karabelas, A. J. Drop Size Spectra Generated in Turbulent Pipe Flow of Dilute Liquid/Liquid Dispersion. *AIChE J.* **1978**, *24(1)*, 170-180.

Kolmogoroff, A. N. About Breaking of Drops in Turbulent Flow. *Dokl. Akad. Nauk. SSSR* **1949**, *66*, 825.

Levich, V. G. *Physicochemical Hydrodynamics*; Prentice Hall: Eaglewood Cliffs, 1962, Chapter 8.

Lissant, K. J., *Emulsions and Emulsion Technology*; Marcel Dekker: New York, 1974; Vol 6, Part 1, Chapter 1.

Liu, G. A Mathematical Model for Prediction of Downhole Gas Well Uniform Corrosion in CO_2 and H_2S Containing Brines; Ph.D. Thesis, Oklahoma State University, Dec. 1991.

Mao, M. L.; Marsden, S. S. Stability of Concentrated Crude Oil-In-Water Emulsions as a Function of Shear Rate, Temperature and Oil Concentration. *J. Can. Pet. Technol.* **1977**, *16*, 54-59.

Quinn, J. A.; Sigloh, D. B. Phase Inversion in the Mixing of Immicible Liquids. *Can. J. Chem. Engng* **1963**, *41*, 15-18.

Robertson, C. A. Down*Hole Phase I: A Computer Model for Predicting the Water Phase Corrosion Zone in Gas and Condensate Wells; Master Thesis, Oklahoma State University, July 1988.

Sambasivam, S. A Model to Predict Oil/Water Emulsion Phase Inversion in the Downhole Environment; Master Thesis, Oklahoma State University, 1994.

Schwarz, N.; Bezemer, C. A New Equation for the Size Distribution of Emulsion Particles. *C. Kolloid Zeitschrift* **1956**, *146*, 139-144.

Selker, A. H.; Sleicher, C. A. Factors Affecting Which Phase Will Disperse When Immicible Liquids Are Stirred Together. *Can. J. Chem. Engng.* **1965**, *43*, 298-301.

Shinoda, K.; Kunieda, H. *Encyclopedia of Emulsion Technology*; Marcel Dekker: New York, 1983; p 337

Shock, D. A.; Sudbury, J. D. Prediction of Corrosion in Oil and Gas Wells. *World Oil* **1951**, *133*, 180-192.

Sibree, J. O. The Viscosity of Emulsions. Part II. *Trans. Faraday Soc.* **1931**, *27*, 161-175.

Simon, R.; Poynter, W. G. Down-Hole Emulsification for Improving Viscous Crude Production. *J. Pet. Tech.* **1968**, *20*, 1349-1353.

Smith, D. H.; Covatch, G. C.; Lim, K. H. Temperature Dependence of Emulsion Morphologies and the Dispersion Morphology Diagram. *J. Phys. Chem.* **1991**, *95(3)*, 1463-1466.

Taylor, G. I. Viscosity of a Fluid Containing Small Drops of Another Fluid. *Proceedings of the Royal Society* **1932**, *201 A*, 192-197.

Tuttle, R. N. Corrosion in Oil and Gas Production. *J. Pet. Tech.* **1987**, *39*, 756-762.

Tuttle, R. N.; Hamby, T. W. Deep Wells-A Corrosion Engineering Challenge. *Material Performance* **1977**, *16(10)*, 9-12.

Stone, H. A. Dynamics of Drop Deformation and Breakup in Viscous Fluids. *Annu. Rev. Fluid Mech.* **1994**, *26*, 65- 102.

APPENDICES

APPENDIX A

NOMENCLATURE

a	maximum velocity gradient in flow field
d	droplet diameter
$d_{combine}$	diameter of the droplet resulting from coalescence of two droplets
d_{ini}	initial droplet diameter
d_{max}	maximum diameter
d_{min}	minimum diameter
k	constant in equation III-7
k_f	a numerical constant in equatin II-5
L	number of trials in which event A occur
N	number of trials
p	probability that event A occurs (eqn. II-7) probability of droplet breakup (eqn. III-6)
p_1	probability of droplet breakup which accounts for the effect of droplet size and flow conditions
p_2	probability of droplet breakup which accounts for the effect of viscosity
Re_l	Reynolds number of the liquid
V	average velocity of the liquid

$V_{lattice}$	volume of the lattice used in simulation
We	Weber number
We_{crit}	critical Weber number
X_{new}	new x-coordinate of droplet
X_{old}	initial x-coordinate of droplet
Y_{new}	new y-coordinate of droplet
Y_{old}	initial y-coordinate of droplet
Z_{new}	new z-coordinate of droplet
Z_{old}	initial z-coordinate of droplet

Greek Symbols

σ	interfacial tension
τ	turbulent stresses
ε	local energy dissipation per unit mass
ν	kinematic viscosity
ρ	density of liquid (eqn. II-5)
ρ_c	density of continuous phase
ρ_l	density of the liquid film
δ	error of the Monte Carlo method (eqn. II-7)
	maximum allowable droplet displacement inside the lattice (eqn. III-2,3,4)
	thickness of the liquid film (eqn. III-8)
ϕ	volume fraction of the dispersed phase

μ_c	viscosity of the continuous phase
μ_d	viscosity of the dispersed phase
μ_l	viscosity of the liquid film
λ_0	scale of eddy at which Reynolds number is unity
υ_0	characteristic eddy velocity
ε_1, ε_2, ε_3	random numbers

APPENDIX B

PROCEDURE FOR RUNNING THE COMPUTER CODE

The computer program for phase inversion prediction is written in FORTRAN (Appendix C). The output from the program is written into three files: DROP.OUT, ENERGY.OUT, and COORD.OUT. DROP.OUT contains the equilibrium drop size distribution. ENERGY.OUT contains the energy of the droplets in a 100-move increment. COORD.OUT contains the coordinates of all droplets in the lattice.

The input variables are given below:

- dmax: maximum droplet diameter
- dmin: minimum droplet diameter
- pwat: volume fraction of water
- visoil: viscosity of oil
- viswat: viscosity of water
- reynolds: reynolds number of liquid
- iter: number of iteration (100,000 to 200,000) is recommended.

To compile the program using RS6000 machines (located in Engineering North 301 and 516), type the following command:

xlf -o *executable file source file*

where *executable file* is the name of the executable file chosen by the user and *source file* is the name of the source code file.

To run the program in the background (recommended), type the following command:

nice nohup *executable file* &

APPENDIX C

COMPUTER CODE TO PREDICT PHASE INVERSION

```
C***  THIS PROGRAM IS USED TO CALCULATE THE ENERGY LEVEL OF WATER-IN-OIL
C     AND OIL-IN-WATER EMULSIONS.  THE EMULSION WITH A LOWER ENERGY IS
C     THE STABLE AND FAVORED EMULSION.  SIMULATION STARTS WITH WATER-IN-
C     OIL EMULSION, THEN FOLLOWS BY OIL-IN-WATER EMULSION.
C     THE INPUT VARIABLES IN THIS PROGRAM ARE:
C           DMAX = MAXIMUM DIAMETER IN THE EMULSION
C           DMIN = MINIMUM DIAMETER IN THE EMULSION
C           PWAT = VOLUME FRACTION OF WATER
C           VISOIL = VISCOSITY OF OIL
C           VISWAT = VISCOSITY OF WATER
C           ITER = NUMBER OF ITERATION
C           REYNOLDS = REYNOLDS NUMBER OF THE LIQUID PHASE
C***

      DOUBLEPRECISION DMAX, DMIN, SIDE, ENERGY
      DOUBLEPRECISION XNEW,YNEW,ZNEW,DMEAN,FINAL_ENG1,FINAL_ENG2
      DOUBLEPRECISION DIA(50000), X(50000), Y(50000), Z(50000)
      DOUBLEPRECISION PHI, MASS, INI_MASS, DIST, VTOT
      INTEGER N, NMOV, COUNT, FCOALESCE, FBREAK
      INTEGER  ITER,EMUL_TYPE
      INTEGER TOT_ITER, SEED,SEED1,SEED2,PRINT_RESULT
      REAL PWAT,PDISP,VISDISP,VISCONT,VISWAT,VISOIL,REYNOLDS
      INTEGER INC_ENERGY, PRINT_ENERGY

C***  THERE ARE 6084 DROPLETS IN THE CUBE INITIALLY.

      FCOALESCE = 0
      FBREAK = 0
      PHI = 3.141592654
      PRINT_ENERGY = 0

      OPEN (UNIT=8, FILE = 'DROP.OUT', STATUS = 'NEW')
      OPEN (UNIT=9, FILE = 'ENERGY.OUT', STATUS = 'NEW')
      OPEN (UNIT=10,FILE = 'COORD.OUT', STATUS = 'NEW')

      PWAT = 0.62

3     DMAX = 18.21
      DMIN = 0.1
      VISWAT = 1.0
      VISOIL = 0.01
      REYNOLDS = 1000.0
```

```
      WRITE(8,180)PWAT
180   FORMAT('VOLUME % OF THE WATER IS ',F5.3)

      TOT_ITER = 200000
      SEED = 869696
      SEED1= 386754
      SEED2= 985872


      EMUL_TYPE = 1

      IF (EMUL_TYPE.EQ.1) THEN

            PDISP = PWAT
            VISDISP = VISWAT
            VISCONT = VISOIL

      ENDIF

2     IF (EMUL_TYPE.EQ.2) THEN

            PDISP = 1.0 - PWAT
            VISDISP = VISOIL
            VISCONT = VISWAT

      ENDIF

      N = 6084

      INC_ENERGY = 1

      DMEAN = 0.3*DMAX

      CALL INITIALIZE_ARRAY(DIA,X,Y,Z)

      CALL CUBE_SIZE(PDISP,DMEAN,SIDE,VTOT)

      CALL PLACE_DROPLET(SIDE,DMEAN,DIA,X,Y,Z)

      CALL CALC_MASS(N,DIA,MASS)

      INI_MASS = MASS

      WRITE(8,*)'&&&&&&&&&&&&&&&&&&&&&&&&&&&&&&&&&&&&&&&&&&&&&&&&&&&&&&&'
      WRITE(8,110) EMUL_TYPE
      WRITE(8,120) INI_MASS

110   FORMAT('EMULSION TYPE IS ',I2)
120   FORMAT('INITIAL MASS = ',E15.7)

      CALL ENERGY_CONFIGURATION(DIA,ENERGY)

      WRITE(8,156) ENERGY/VTOT
156   FORMAT('INITIAL ENERGY OF THE SYSTEM IS ',E15.5)
```

```
      ITER = 0

1     ITER = ITER + 1


      CALL MOVE_DROPLET(N,DIA,SIDE,X,Y,Z,XNEW,YNEW,ZNEW,NMOV,SEED,
     &                  DMAX)

      CALL COALESCENCE(X,Y,Z,DIA,XNEW,YNEW,ZNEW,N,NMOV,DMAX,
     &                   SEED1,FCOALESCE)

      CALL BREAKUP(N,DIA,DMAX,DMIN,X,Y,Z,SEED2,SEED1,FBREAK,SIDE,
     &             FCOALESCE,DMEAN,VISDISP,VISCONT,REYNOLDS)

      IF (ITER.EQ.(100*INC_ENERGY)) PRINT_ENERGY=1

      IF (PRINT_ENERGY.EQ.1) THEN

            CALL ENERGY_CONFIGURATION(DIA,ENERGY)
            WRITE(9,155) ITER, ENERGY/VTOT
155         FORMAT(I8,5X,E14.7)
            INC_ENERGY = INC_ENERGY+1
            PRINT_ENERGY = 0

      ENDIF


C     IF (ITER.EQ.500) PRINT_RESULT = 1
C     IF (ITER.EQ.1000) PRINT_RESULT = 1
C     IF (ITER.EQ.5000) PRINT_RESULT = 1
C     IF (ITER.EQ.10000) PRINT_RESULT = 1
C     IF (ITER.EQ.50000) PRINT_RESULT = 1
C     IF (ITER.EQ.70000) PRINT_RESULT = 1
C     IF (ITER.EQ.100000) PRINT_RESULT = 1
C     IF (ITER.EQ.150000) PRINT_RESULT = 1
      IF (ITER.EQ.200000) PRINT_RESULT = 1
      IF (ITER.EQ.300000) PRINT_RESULT = 1
      IF (ITER.EQ.TOT_ITER) PRINT_RESULT = 1

      IF (PRINT_RESULT.EQ.1) THEN

            CALL CALC_MASS(N,DIA,MASS)
            WRITE(8,970) MASS
970         FORMAT('MASS=',E15.7)
            DIST = 0.71
            CALL SORT_DROPLET(DIA,DIST,DMIN,DMAX,ITER)
            PRINT_RESULT = 0
            WRITE(8,980) FCOALESCE, FBREAK
980         FORMAT('FCOALESCE=',I8,2X,'FBREAK=',I8)

      ENDIF

      IF(ITER.LT.TOT_ITER) THEN
```

```
            GOTO 1
      ENDIF

      DO 333 COUNT = 1,50000
            WRITE(10,334) X(COUNT),Y(COUNT),Z(COUNT)
333   CONTINUE
334   FORMAT(F10.5,5X,F10.5,5X,F10.5)


      IF (EMUL_TYPE.EQ.1) THEN

            CALL ENERGY_CONFIGURATION(DIA,ENERGY)
            FINAL_ENG1 = ENERGY/VTOT
            WRITE(8,130) FINAL_ENG1
            EMUL_TYPE = 2
            GOTO 2

      ENDIF

      IF (EMUL_TYPE.EQ.2) THEN

            CALL ENERGY_CONFIGURATION(DIA,ENERGY)
            FINAL_ENG2 = ENERGY/VTOT
            WRITE(8,140) FINAL_ENG2

      ENDIF

130   FORMAT('ENERGY AT EQUILIBRIUM FOR WATER IN OIL = ',E15.8)
140   FORMAT('ENERGY AT EQUILIBRIUM FOR OIL IN WATER = ',E15.8)

      IF (PWAT.LE.0.56) STOP

      IF (FINAL_ENG2.LT.FINAL_ENG1) THEN

            WRITE(8,*) 'PHASE INVERSION OCCURRED'
            PWAT = PWAT - 0.02
            GOTO 3

      ELSE

            WRITE(8,*) 'NO PHASE INVERSION'
            PWAT = PWAT - 0.02
            GOTO 3

      ENDIF


      STOP
      END


C*********************************************************************
      SUBROUTINE INITIALIZE_ARRAY(DIA,X,Y,Z)
      DOUBLEPRECISION DIA(50000), X(50000), Y(50000), Z(50000)
```

```
      INTEGER COUNT

C***  THIS SUBROUTINE IS USED TO INITIALIZE ALL ARRAYS TO ZERO.

      DO 10 COUNT = 1, 50000
            DIA(COUNT) = 0.0
            X(COUNT) = 0.0
            Y(COUNT) = 0.0
            Z(COUNT) = 0.0
10    CONTINUE

      RETURN
      END
C ***********************************************************************
      SUBROUTINE CUBE_SIZE(PDISP,DMEAN,SIDE,VTOT)
      DOUBLEPRECISION DMEAN,SIDE,PHI,VOL_DROP,VTOT
      REAL PDISP
      INTEGER TOT_DROP


C***  THIS SUBROUTINE CALCULATE THE SIZE OF THE CUBE WITH 6084 DROPLETS
C***  INSIDE FOR THE GIVEN VOLUME FRACTION OF WATER.
C***  SIDE = THE SIDE OF THE CUBE, CM

      TOT_DROP = 6084
      PHI = 3.141592654
      VOL_DROP = TOT_DROP/6.0*PHI*DMEAN**3
      VTOT = VOL_DROP/PDISP
      SIDE = VTOT**(1.0/3.0)

      RETURN
      END
C***********************************************************************
      SUBROUTINE PLACE_DROPLET(SIDE,DMEAN,DIA,X,Y,Z)
      DOUBLE PRECISION DIA(50000),X(50000),Y(50000),Z(50000)
      DOUBLE PRECISION SIDE,DMEAN,CONST
      INTEGER COUNT, NDR, I, J, K

C***  THIS SUBROUTINE PLACES DROPLETS IN THE LATTICE IN A FACE CUBIC
C     CENTER CONFIGURATION.
C***  NDR = NUMBER OF DROPLET ON THE SIDE OF THE CUBE.
C***  A TOTAL OF 6084 DROPLETS ARE PLACED IN THE CUBE INITIALLY WITH
C     NDR = 12.

      NDR = 12
      COUNT = 1
      CONST = SIDE/(2.0*(NDR-1.0))
      DO 10 I = 1, NDR
      DO 20 J = 1, NDR
      DO 30 K = 1, NDR
            X(COUNT) = (REAL(I)-1.0)*SIDE/(NDR-1)
            Y(COUNT) = (REAL(J)-1.0)*SIDE/(NDR-1)
            Z(COUNT) = (REAL(K)-1.0)*SIDE/(NDR-1)
            DIA(COUNT) = DMEAN
```

```
            COUNT = COUNT + 1
30      CONTINUE
20      CONTINUE
10      CONTINUE

        DO 40 I = 1, NDR-1
        DO 50 J = 1, NDR-1
        DO 60 K = 1, NDR
              X(COUNT) = REAL(I)*SIDE/(NDR-1)-CONST
              Y(COUNT) = REAL(J)*SIDE/(NDR-1)-CONST
              Z(COUNT) = (REAL(K)-1.0)*SIDE/(NDR-1)
              DIA(COUNT) = DMEAN
              COUNT = COUNT + 1
60      CONTINUE
50      CONTINUE
40      CONTINUE

        DO 70 I = 1, NDR-1
        DO 80 J = 1, NDR
        DO 90 K = 1, NDR-1
              X(COUNT) = REAL(I)*SIDE/(NDR-1)-CONST
              Y(COUNT) = (REAL(J)-1.0)*SIDE/(NDR-1)
              Z(COUNT) = REAL(K)*SIDE/(NDR-1)-CONST
              DIA(COUNT) = DMEAN
              COUNT = COUNT+1
90      CONTINUE
80      CONTINUE
70      CONTINUE

        DO 100 I = 1, NDR
        DO 110 J = 1, NDR-1
        DO 120 K = 1, NDR-1
              X(COUNT) = (REAL(I)-1.0)*SIDE/(NDR-1)
              Y(COUNT) = REAL(J)*SIDE/(NDR-1)-CONST
              Z(COUNT) = REAL(K)*SIDE/(NDR-1)-CONST
              DIA(COUNT) = DMEAN
              COUNT = COUNT + 1
120     CONTINUE
110     CONTINUE
100     CONTINUE

        RETURN
        END
C*********************************************************************
        SUBROUTINE ENERGY_CONFIGURATION(DIA,ENERGY)
        DOUBLEPRECISION DIA(50000), PHI, ENERGY, SUM
        INTEGER COUNT
        REAL SURF_TENS

C***    THIS SUBROUTINE CALCULATES THE ENERGY OF THE DROPLETS IN THE
C       LATTICE.

        SUM = 0.0
        PHI = 3.141592654
```

```
      SURF_TENS = 30
      DO 10 COUNT = 1,50000
            SUM = SUM + DIA(COUNT)**2
10    CONTINUE
      ENERGY = PHI*SUM*SURF_TENS

      RETURN
      END
C*********************************************************************
      SUBROUTINE MOVE_DROPLET(N,DIA,SIDE,X,Y,Z,XNEW,YNEW,ZNEW,NMOV,
     &                        SEED,DMAX)
      DOUBLEPRECISION DIA(50000),SIDE, X(50000),Y(50000),Z(50000)
      DOUBLEPRECISION XNEW,YNEW,ZNEW,DRMAX,DMAX
      REAL JJ, RANDX
      INTEGER NMOV,SEED,N

C***  THIS SUBROUTINE MOVES A DROPLET RANDOMLY INSIDE THE LATTICE.
C     IF THE DROPLET MOVES OUT FROM THE LATTICE, IT IS MOVED BACK INSIDE
C     THE LATTICE.

10    NMOV = 0
      JJ = 0.0
      CALL RANDOM(SEED,RANDX)
            JJ = N*RANDX
            NMOV = ANINT(JJ)
      IF (NMOV.EQ.0) GOTO 10
      IF (DIA(NMOV).EQ.0.0) GOTO 10

C***  MOVE DROPLET NMOV RANDOMLY.

      DRMAX = 0.1*DMAX

      CALL RANDOM(SEED,RANDX)
      XNEW = X(NMOV) + (2.0*RANDX-1.0)*DRMAX
      CALL RANDOM(SEED,RANDX)
      YNEW = Y(NMOV) + (2.0*RANDX-1.0)*DRMAX
      CALL RANDOM(SEED,RANDX)
      ZNEW = Z(NMOV) + (2.0*RANDX-1.0)*DRMAX

      IF (XNEW.LT.0) XNEW = -XNEW
      IF (XNEW.GT.SIDE) XNEW = 2*SIDE-XNEW
      IF (YNEW.LT.0) YNEW = -YNEW
      IF (YNEW.GT.SIDE) YNEW = 2*SIDE-YNEW
      IF (ZNEW.LT.0) ZNEW = -ZNEW
      IF (ZNEW.GT.SIDE) ZNEW = 2*SIDE-ZNEW

      RETURN
      END
C*********************************************************************
      SUBROUTINE COALESCENCE(X,Y,Z,DIA,XNEW,YNEW,ZNEW,N,
     &                       NMOV,DMAX,SEED1,FCOALESCE)
      DOUBLE PRECISION X(50000), Y(50000), Z(50000), DIA(50000)
      DOUBLEPRECISION XNEW, YNEW, ZNEW, RCRIT, D2, DMAX
      DOUBLEPRECISION DBREAK
```

```
      INTEGER N, NMOV, JJ
      INTEGER NEIGH, SEED1,FCOALESCE,COA
      REAL RANDX1

C***  THIS SUBROUTINE CHECKS IF A DROPLET COALESCE WITH ITS NEIGHBOUR.
C     IF THE DROPLET COALESCES WITH ANOTHER, THE DIAMETER OF THE NEW
C     DROPLET IS CALCULATED.

      NEIGH = 0

C***  CHECK IF DROPLET NMOV WILL COALESCE WITH ITS NEIGHBOUR.

      DO 10 JJ = 1,N
            IF (JJ.EQ.NMOV) GOTO 10
            IF (DIA(JJ).EQ.0.0) GOTO 10
            RCRIT = 0.3*(DIA(NMOV)+DIA(JJ))
            IF (ABS(XNEW-X(JJ)).GT.RCRIT) GOTO 10
            IF (ABS(YNEW-Y(JJ)).GT.RCRIT) GOTO 10
            IF (ABS(ZNEW-Z(JJ)).GT.RCRIT) GOTO 10
            NEIGH = JJ
            GOTO 20
10    CONTINUE

C***  DROPLET NMOV DID NOT COALESCE WITH ITS NEIGHBOUR,ENERGY REMAIN THE
C     SAME.  PLACE THE DROPLET TO ITS NEW POSITION.

      X(NMOV) = XNEW
      Y(NMOV) = YNEW
      Z(NMOV) = ZNEW
      GOTO 30

C***  DROPLET NMOV COALESCED WITH ITS NEIGHBOUR, CHECK IF THE RESULTING
C***  SIZE EXCEEDS THE MAXIMUM DIAMETER.

20    D2 = (DIA(NMOV)**3+DIA(NEIGH)**3)**(1.0/3.0)

      IF (D2.LE.DMAX) THEN

            DIA(NMOV) = 0.0
            X(NMOV) = 0.0
            Y(NMOV) = 0.0
            Z(NMOV) = 0.0
            DIA(NEIGH) = D2

C***  REPLACE THE DROPLET DELETED WITH THE LAST DROPLET FROM THE ARRAY.

            IF (NMOV.NE.N) THEN

                  DIA(NMOV) = DIA(N)
                  X(NMOV) = X(N)
                  Y(NMOV) = Y(N)
                  Z(NMOV) = Z(N)

C***  DELETE THE LAST DROPLET FROM THE ARRAY.
```

```
                DIA(N) = 0.0
                X(N) = 0.0
                Y(N) = 0.0
                Z(N) = 0.0

            ENDIF

        N = N-1
        FCOALESCE = FCOALESCE+1

        ENDIF

C***    IF THE DIAMETER RESULTING FROM COALESCENCE IS GREATER THAN THE
C***    MAXIMUM DIAMETER, THE DROPLET BREAKS INTO TWO, ONE OF THEM WITH
C***    DIAMETER EQUAL TO MAXIMUM DIAMETER.

        IF (D2.GT.DMAX) THEN

            DIA(NEIGH) = DMAX
            DIA(NMOV)  = (D2**3-DMAX**3)**(1.0/3.0)

        ENDIF


30      RETURN
        END
C*****************************************************************************
        SUBROUTINE BREAKUP(N,DIA,DMAX,DMIN,X,Y,Z,SEED2,
       &    SEED1,FBREAK,SIDE,FCOALESCE,DMEAN,VISDISP,VISCONT,REYNOLDS)


        INTEGER N,MM,NBRE
        INTEGER SEED1,SEED2,FBREAK,FCOALESCE,BRE,NNEW
        REAL KK,RANDX2,VISDISP,VISCONT,CONSTANT,REYNOLDS
        DOUBLEPRECISION DIA(50000),X(50000),Y(50000),Z(50000)
        DOUBLEPRECISION DB, DMAX, DMIN
        DOUBLEPRECISION PROB, PROB1, PROB2, SIDE
        DOUBLEPRECISION DMEAN,RRCRIT,XXNEW,YYNEW,ZZNEW

C***    THIS SUBROUTINE CALCULATES THE PROBABILITY OF DROPLET BREAKUP.
C       IF THE PROBABILITY OF BREAKUP IS HIGHER THAN A RANDOM NUMBER, THE
C       DROPLET IS ALLOWED TO BREAK.

120     KK = 0.0
        NBRE = 0
        CALL RANDOM2(SEED2,RANDX2)
        KK = N*RANDX2
        NBRE = ANINT(KK)

        IF (NBRE.EQ.0) GOTO 120
        IF (DIA(NBRE).EQ.0.0) GOTO 120

        CONSTANT =  EXP(-1000.0/REYNOLDS)
        PROB1 =  EXP(-(VISDISP/VISCONT))
```

```
      PROB2 = CONSTANT *((DIA(NBRE)-DMIN)/(DMAX-DMIN))
      PROB  = 0.5*(PROB1+PROB2)

      DB = DIA(NBRE)*0.5**(1.0/3.0)

      CALL RANDOM2(SEED2,RANDX2)

      BRE = 0

C***  IF THE SIZE OF THE DROPLET RESULTING FROM THE BREAKUP IS LESS THAN
C***  THE MINIMUM DIAMETER, DROPLET BREAKUP IS REJECTED.

      IF(RANDX2.LT.PROB) THEN

            IF (DB.LT.DMIN) THEN
                  BRE = 0
            ELSE
                  BRE = 1
            ENDIF

      ELSE

            BRE = 0

      ENDIF

      IF (BRE.EQ.1) THEN

            DIA(NBRE) = DB

C***        THE NEW DROPLET FORMED FROM THE BREAKUP IS PLACED AT THE
C***        END OF THE ARRAY.

            NNEW = N+1
20          DIA(NNEW) = DB

C***  THE DROPLET CREATED FROM BREAKUP IS PLACED RANDOMLY INSIDE THE
C***  LATTICE.

            CALL RANDOM2(SEED2,RANDX2)
            X(NNEW)= RANDX2*SIDE
            XXNEW = X(NNEW)
            CALL RANDOM2(SEED2,RANDX2)
            Y(NNEW)= RANDX2*SIDE
            YYNEW = Y(NNEW)
            CALL RANDOM2(SEED2,RANDX2)
            Z(NNEW)= RANDX2*SIDE
            ZZNEW = Z(NNEW)

            FBREAK = FBREAK+1
            N = N + 1

C***        THE DROPLET RESULTING FROM THE BREAKUP IS CHECKED FOR THE
C           POSSIBILITY OF COALESCENCE WHEN PLACED RANDOMLY INSIDE THE
```

```
C***        LATTICE

            CALL COALESCENCE(X,Y,Z,DIA,XXNEW,YYNEW,ZZNEW,N,NNEW,
     &                  DMAX,SEED1,FCOALESCE)

      ENDIF

      RETURN
      END


C*********************************************************************
      SUBROUTINE CALC_MASS(N,DIA,MASS)

      DOUBLEPRECISION DIA(50000), MASS, SUM, PHI
      INTEGER N, COUNT
      REAL DENSITY

C***  THIS SUBROUTINE CALCULATES THE TOTAL MASS OF DROPLETS IN THE
C     EMULSION.

      PHI = 3.141592654
      DENSITY = 1.0
      SUM = 0
      MASS = 0.0

      DO 100 COUNT = 1,N
            SUM = SUM + DIA(COUNT)**3
100   CONTINUE

      MASS = DENSITY*SUM*PHI/6.0

      RETURN
      END
C*********************************************************************
      SUBROUTINE SORT_DROPLET(DIA,DIST,DMIN,DMAX,ITER)

      DOUBLEPRECISION DIA(50000),DIST,DMIN,DMAX
      INTEGER RANGE1,RANGE2,RANGE3,RANGE4,RANGE5,RANGE6,RANGE7
      INTEGER RANGE8,RANGE9,RANG10, RANGEMIN,RANGEMAX, TOTDROP,ITER
      INTEGER RANG11,RANG12,RANG13,RANG14,RANG15,RANG16,RANG17,RANG18
      INTEGER RANG19,RANG20,RANG21,RANG22,RANG23,RANG24,RANG25,RANG26
      INTEGER RANG27,RANG28,RANG29,RANG30,RANG31,RANG32,RANG33,RANG34
      INTEGER RANG35,RANG36,RANG37,RANG38,RANG39,RANG40
      INTEGER COUNT

C***  THIS SUBROUTINE SORTS THE DROPLETS IN A CERTAIN SIZE RANGE.

      RANGE1 = 0
      RANGE2 = 0
      RANGE3 = 0
      RANGE4 = 0
      RANGE5 = 0
      RANGE6 = 0
```

```
RANGE7 = 0
RANGE8 = 0
RANGE9 = 0
RANG10 = 0
RANG11 = 0
RANG12 = 0
RANG13 = 0
RANG14 = 0
RANG15 = 0
RANG16 = 0
RANG17 = 0
RANG18 = 0
RANG19 = 0
RANG20 = 0
RANG21 = 0
RANG22 = 0
RANG23 = 0
RANG24 = 0
RANG25 = 0
RANG26 = 0
RANG27 = 0
RANG28 = 0
RANG29 = 0
RANG30 = 0
RANG31 = 0
RANG32 = 0
RANG33 = 0
RANG34 = 0
RANG35 = 0
RANG36 = 0
RANG37 = 0
RANG38 = 0
RANG39 = 0
RANG40 = 0
RANGEMIN = 0
RANGEMAX = 0
TOTDROP = 0


DO 10 COUNT = 1, 50000
      IF (DIA(COUNT).NE.0.0) THEN
      IF (DIA(COUNT).NE.0) TOTDROP = TOTDROP+1
      IF (DIA(COUNT).LT.DMIN) RANGEMIN= RANGEMIN+1
      IF (DIA(COUNT).LT.(1.*DIST)) RANGE1= RANGE1+1
      IF (DIA(COUNT).LT.(2.*DIST)) RANGE2= RANGE2+1
      IF (DIA(COUNT).LT.(3.*DIST)) RANGE3= RANGE3+1
      IF (DIA(COUNT).LT.(4.*DIST)) RANGE4= RANGE4+1
      IF (DIA(COUNT).LT.(5.*DIST)) RANGE5= RANGE5+1
      IF (DIA(COUNT).LT.(6.*DIST)) RANGE6= RANGE6+1
      IF (DIA(COUNT).LT.(7.*DIST)) RANGE7= RANGE7+1
      IF (DIA(COUNT).LT.(8.*DIST)) RANGE8= RANGE8+1
      IF (DIA(COUNT).LT.(9.*DIST)) RANGE9= RANGE9+1
      IF (DIA(COUNT).LT.(10.*DIST))RANG10= RANG10+1
      IF (DIA(COUNT).LT.(11.*DIST))RANG11= RANG11+1
```

```
            IF (DIA(COUNT).LT.(12.*DIST))RANG12= RANG12+1
            IF (DIA(COUNT).LT.(13.*DIST))RANG13= RANG13+1
            IF (DIA(COUNT).LT.(14.*DIST))RANG14= RANG14+1
            IF (DIA(COUNT).LT.(15.*DIST))RANG15= RANG15+1
            IF (DIA(COUNT).LT.(16.*DIST))RANG16= RANG16+1
            IF (DIA(COUNT).LT.(17.*DIST))RANG17= RANG17+1
            IF (DIA(COUNT).LT.(18.*DIST))RANG18= RANG18+1
            IF (DIA(COUNT).LT.(19.*DIST))RANG19= RANG19+1
            IF (DIA(COUNT).LT.(20.*DIST))RANG20= RANG20+1
            IF (DIA(COUNT).LT.(21.*DIST))RANG21= RANG21+1
            IF (DIA(COUNT).LT.(22.*DIST))RANG22= RANG22+1
            IF (DIA(COUNT).LT.(23.*DIST))RANG23= RANG23+1
            IF (DIA(COUNT).LT.(24.*DIST))RANG24= RANG24+1
            IF (DIA(COUNT).LT.(25.*DIST))RANG25= RANG25+1
            IF (DIA(COUNT).LT.(26.*DIST))RANG26= RANG26+1
            IF (DIA(COUNT).LT.(27.*DIST))RANG27= RANG27+1
            IF (DIA(COUNT).LT.(28.*DIST))RANG28= RANG28+1
            IF (DIA(COUNT).LT.(29.*DIST))RANG29= RANG29+1
            IF (DIA(COUNT).LT.(30.*DIST))RANG30= RANG30+1
            IF (DIA(COUNT).LT.(31.*DIST))RANG31= RANG31+1
            IF (DIA(COUNT).LT.(32.*DIST))RANG32= RANG32+1
            IF (DIA(COUNT).LT.(33.*DIST))RANG33= RANG33+1
            IF (DIA(COUNT).LT.(34.*DIST))RANG34= RANG34+1
            IF (DIA(COUNT).LT.(35.*DIST))RANG35= RANG35+1
            IF (DIA(COUNT).LT.(36.*DIST))RANG36= RANG36+1
            IF (DIA(COUNT).LT.(37.*DIST))RANG37= RANG37+1
            IF (DIA(COUNT).LT.(38.*DIST))RANG38= RANG38+1
            IF (DIA(COUNT).LT.(39.*DIST))RANG39= RANG39+1
            IF (DIA(COUNT).LT.(40.*DIST))RANG40= RANG40+1
            IF (DIA(COUNT).GT.DMAX) RANGEMAX = RANGEMAX+1

      ENDIF
10    CONTINUE

      WRITE(8,*)'*************************************************'
      WRITE(8,18) ITER
      WRITE(8,19) DMIN,RANGEMIN
      WRITE(8,199) (1.*DIST), RANGE1
      WRITE(8,20) (1.*DIST),(2.*DIST),(RANGE2-RANGE1)
      WRITE(8,20) (2.*DIST),(3.*DIST),(RANGE3-RANGE2)
      WRITE(8,20) (3.*DIST),(4.*DIST),(RANGE4-RANGE3)
      WRITE(8,20) (4.*DIST),(5.*DIST),(RANGE5-RANGE4)
      WRITE(8,20) (5.*DIST),(6.*DIST),(RANGE6-RANGE5)
      WRITE(8,20) (6.*DIST),(7.*DIST),(RANGE7-RANGE6)
      WRITE(8,20) (7.*DIST),(8.*DIST),(RANGE8-RANGE7)
      WRITE(8,20) (8.*DIST),(9.*DIST),(RANGE9-RANGE8)
      WRITE(8,20) (9.*DIST),(10.*DIST),(RANG10-RANGE9)
      WRITE(8,20) (10.*DIST),(11.*DIST),(RANG11-RANG10)
      WRITE(8,20) (11.*DIST),(12.*DIST),(RANG12-RANG11)
      WRITE(8,20) (12.*DIST),(13.*DIST),(RANG13-RANG12)
      WRITE(8,20) (13.*DIST),(14.*DIST),(RANG14-RANG13)
      WRITE(8,20) (14.*DIST),(15.*DIST),(RANG15-RANG14)
      WRITE(8,20) (15.*DIST),(16.*DIST),(RANG16-RANG15)
      WRITE(8,20) (16.*DIST),(17.*DIST),(RANG17-RANG16)
```

```
      WRITE(8,20) (17.*DIST),(18.*DIST),(RANG18-RANG17)
      WRITE(8,20) (18.*DIST),(19.*DIST),(RANG19-RANG18)
      WRITE(8,20) (19.*DIST),(20.*DIST),(RANG20-RANG19)
      WRITE(8,20) (20.*DIST),(21.*DIST),(RANG21-RANG20)
      WRITE(8,20) (21.*DIST),(22.*DIST),(RANG22-RANG21)
      WRITE(8,20) (22.*DIST),(23.*DIST),(RANG23-RANG22)
      WRITE(8,20) (23.*DIST),(24.*DIST),(RANG24-RANG23)
      WRITE(8,20) (24.*DIST),(25.*DIST),(RANG25-RANG24)
      WRITE(8,20) (25.*DIST),(26.*DIST),(RANG26-RANG25)
      WRITE(8,20) (26.*DIST),(27.*DIST),(RANG27-RANG26)
      WRITE(8,20) (27.*DIST),(28.*DIST),(RANG28-RANG27)
      WRITE(8,20) (28.*DIST),(29.*DIST),(RANG29-RANG28)
      WRITE(8,20) (29.*DIST),(30.*DIST),(RANG30-RANG29)
      WRITE(8,20) (30.*DIST),(31.*DIST),(RANG31-RANG30)
      WRITE(8,20) (31.*DIST),(32.*DIST),(RANG32-RANG31)
      WRITE(8,20) (32.*DIST),(33.*DIST),(RANG33-RANG32)
      WRITE(8,20) (33.*DIST),(34.*DIST),(RANG34-RANG33)
      WRITE(8,20) (34.*DIST),(35.*DIST),(RANG35-RANG34)
      WRITE(8,20) (35.*DIST),(36.*DIST),(RANG36-RANG35)
      WRITE(8,20) (36.*DIST),(37.*DIST),(RANG37-RANG36)
      WRITE(8,20) (37.*DIST),(38.*DIST),(RANG38-RANG37)
      WRITE(8,20) (38.*DIST),(39.*DIST),(RANG39-RANG38)
      WRITE(8,20) (39.*DIST),(40.*DIST),(RANG40-RANG39)
      WRITE(8,31) DMAX,RANGEMAX
      WRITE(8,30) TOTDROP

18    FORMAT('ITERATION=',I8)
19    FORMAT(14X,'< ',F15.5,'=',I8)
199   FORMAT('0',14X,'-',F15.5,'=',I8)
20    FORMAT(F15.5,'-',F15.5,'=',I8)
30    FORMAT('TOTAL DROPLET LEFT = ', I8)
31F   FORMAT(14X,'> ',F15.5,'=',I8)


      RETURN
      END
C*********************************************************************
      SUBROUTINE RANDOM(SEED, RANDX)

      INTEGER SEED
      REAL RANDX

      SEED = 2045*SEED + 1
      SEED = SEED - (SEED/1048576)*1048576
      RANDX = REAL(SEED + 1) / 1048577.0

      RETURN
      END
C*********************************************************************
      SUBROUTINE RANDOM1(SEED1, RANDX1)

      INTEGER SEED1
      REAL RANDX1
```

```
      SEED1 = 2045*SEED1 + 1
      SEED1 = SEED1 - (SEED1/1048576)*1048576
      RANDX1 = REAL(SEED1 + 1) / 1048577.0

      RETURN
      END
C*****************************************************************************
      SUBROUTINE RANDOM2(SEED2, RANDX2)

      INTEGER SEED2
      REAL RANDX2

      SEED2 = 2045*SEED2 + 1
      SEED2 = SEED2 - (SEED2/1048576)*1048576
      RANDX2 = REAL(SEED2 + 1) / 1048577.0

      RETURN
      END
```

APPENDIX D

Sample Calculations of Droplet Volume and Surface Area

The drop size distribution for Case II after 50,000 and 100,000 moves are given below:

Dia.(micron)	Ave.Dia (micron)	Move = 50,000	Move = 100,000
0-0.71	0.355	4926	22414
0.71-1.42	1.065	4430	6720
1.42-2.13	1.775	2207	2215
2.13-2.84	2.485	1644	1277
2.84-3.55	3.195	832	708
3.55-4.26	3.905	571	474
4.26-4.97	4.615	436	320
4.97-5.68	5.325	348	271
5.68-6.39	6.035	280	196
6.39-7.10	6.745	208	170
7.10-7.81	7.455	162	136
7.81-8.52	8.165	122	133
8.52-9.23	8.875	96	105
9.23-9.94	9.585	75	77
9.94-10.65	10.295	63	46
10.65-11.36	11.005	37	42
11.36-12.07	11.715	35	33
12.07-12.78	12.425	28	23
12.78-13.49	13.135	18	22
13.49-14.20	13.845	13	15
14.20-14.91	14.555	6	19
14.91-15.62	15.265	6	8
15.62-16.33	15.975	3	3
16.33-17.04	16.685	4	5
17.04-17.75	17.395	2	2
17-75-18.46	18.105	3	7
Total Droplets		16555	35441

The simulations were started with 6084 droplets which had initial diameter of 5.463 micron. So, the initial diameter was in the range of 4.97 - 5.68.

The initial volume of droplets
$= 6084 \times \pi/6 \times (5.463)^3 = \underline{519,376}$

The initial surface area of droplets
$= 6084 \times \pi \times (5.463)^2 = \underline{570,429}$

Note: The average diameter was used in the following approximater calculations.

<u>At 50,000 Moves:</u>

1. Number of droplets with diameter less than 5.68 micron = 15,394/16,555 x 100% = <u>93%</u>
   Number of droplets with diameter greater than 5.68 micron = <u>7%</u>

2. Volume of droplets with diameter less than 5.68 micron = $\pi/6$ ($4926 \times 0.355^3 + 4430 \times 1.065^3 + 2207 \times 1.775^3 + 1644 \times 2.485^3 + 832 \times 3.195^3 + 571 \times 3.905^3 + 436 \times 4.615^3 + 348 \times 5.325^3$)
   = 199,680
   = 199,680/519,376 x 100% = <u>38%</u>

   Volume of droplets with diameter greater than 5.68 micron = <u>62%</u>

3. Surface area of droplets with diameter less than 5.68 micron = π ($4926 \times 0.355^2 + 4430 \times 1.065^2 + 2207 \times 1.775^2 + 1644 \times 2.485^2 + 832 \times 3.195^2 + 571 \times 3.905^2 + 436 \times 4615^2 + 348 \times 5.325^2$)
   = <u>185,684</u>

   Surface area of droplets with diameter greater than 5.68 micron
   = π ($280 \times 6.035^2 + 208 \times 6.745^2 + 162 + 7.455^2 + 122 \times 8.165^2 + 96 \times 8.875^2 + 75 \times 9.585^2 + 63 \times 10.295^2 + 37 \times 11.005^2 + 35 \times 11.715^2 + 28 \times 12.425^2 + 18 \times 13.135^2 + 13 \times 13.845^2 + 6 \times 14.555^2 + 6 \times 15.265^2 + 3 \times 15.975^2 + 4 \times 16.685^2 + 2 \times 17.375^2 + 3 \times 18.105^2$)
   = <u>248,795</u>

Total surface area at 50,000 moves
= 185,684+248,795 = 434,479 < 570,429

At 100,000 moves

1. Number of droplets with diameter less than 5.68 micron = 34,399/35,441 x 100% = 97%

Number of droplets with diameter greater than 5.68 micron = 3%

2. Volume of droplets with diameter less than 5.68 micron = $\pi/6$ (22414x0.355^3 +6720x1.065^3 + 2215x1.775^3 + 1277x2.485^3 +708x3.195^3 +474x3.905^3 +320x4.615^3 + 271x5.325^3) = 164,792

= 164,792/519,376 x 100% = 32%

Volume of droplets with diameter greater than 5.68 micron = 68%

3. Surface area of droplets with diameter less than 5.68 micron = π (22,414x0.355^2 + 6720x1.065^2 +2215x1.775 + 1277x2.485^2 + 708x3.195^2 + 474x3.905^2 + 320x4.615^2 + 271x5.325^2) = 154,884

Surface area of droplets with diameter greater than 5.68 micron = π (196x6.035^2 + 170x6.745^2 + 136x7.455^2 + 133x8.165^2 + 105x8.875^2 + 77x9.585^2 + 46x10.295^2 + 42x11.005^2 + 33x11.715^2 + 23x12.425^2 + 22x13.135^2 + 15x13.845^2 + 19x14.555^2 + 8x15.265^2 + 3x15.975^2 + 5x16.685^2 + 2x17.395^2 + 7x18.105^2)

= 258,558

Total surface area at 100,000 moves
= 154,884+258,558 = 413,442 < 570,429

VITA

Justin Juswandi

Candidate for the Degree of

Master of Science

Thesis: SIMULATION OF THE OIL-WATER INVERSION PROCESSES

Major Field: Chemical Engineering

Biographical:

Personal Data: Born in Medan, Indonesia, on September 2, 1970, the son of Jasin and Betty.

Education: Graduated from Sutomo High School, Medan, Indonesia, in May 1989; received Bachelor of Science degree in Chemical Engineering from Oklahoma State University, Stillwater, Oklahoma in May 1993. Completed the requirements for the Master of Science degree in Chemical Engineering at Oklahoma State University in May 1995.

Experience: Undergraduate and graduate research assistant, School of Chemical Engineering, Oklahoma State University, January, 1993 to May, 1995. Undergraduate research assistant, Department of Chemistry, Oklahoma State University, January ,1991 to May, 1991.

Professional Membership: American Institute of Chemical Engineers.